Semisynthetic glycopeptide antibiotics

Groesen, E. van

Chapter 3 |

The guanidino lipoglycopeptides – properties, mechanism of action, and *in vivo* efficacy

Parts of this chapter are under revision as manuscript at *Science Translation Medicine* as:

van Groesen, E., Kotsogianni, I., Arts, M., Tehrani, K.M.H.E., Wade, N., Zwerus, J.T., De Benedetti, S., Bakker, A., Chakraborty, P., van der Stelt, M., Scheffers, D-J., Holden, K., Schneider, T., Martin, N.I. The guanidino lipoglycopeptides: Novel semisynthetic glycopeptides with potent *in vitro* and *in vivo* antibacterial activity. (2022)

Part of the data in this chapter are part of a Dutch Patent:

"Antibacterial Compounds"; Martin, N.I.; van Groesen, E.; Tehrani, K.H.M.E.; Wade, N.; Priority date 24 September 2019; granted 2021; N2023883

3.1 Introduction

The accelerated appearance of multi drug-resistant (MDR) pathogens continues to present a growing threat to modern medicine's capacity to fight infectious diseases. A recent study estimates that in 2019 antimicrobial resistance (AMR) was directly responsible for 1.27 million deaths worldwide and further associated with an estimated 4.95 million deaths.[1] Among the pathogens that contribute most to this global burden of AMR, drug-resistant Gram-positive species *S. aureus* and *S. pneumoniae* are responsible for a combined 0.5 million annual deaths.[1] Historically, treatment of such Gram-positive infections has relied upon the glycopeptide family of antibiotics, typified by vancomycin, as a last line of defense. These glycopeptides bind to the D-Ala-D-Ala terminus of lipid II using five hydrogen bonds, preventing elongation of the polymeric cell wall and eventually resulting in cell wall biosynthesis inhibition.[2–5] In recent years however, vancomycin-resistance has emerged. This phenomenon occurs when the target changes to D-Ala-D-Lac resulting in electrostatic repulsion and reduced binding affinity, which ultimately renders vancomycin inactive.[6–9] The diminished susceptibility of Gram-positive species to last-line therapeutics such as vancomycin highlights the importance of developing next generation glycopeptides with enhanced antibacterial activities and improved safety profiles.

In **Chapter 2** we report the discovery and development of a novel class of highly potent semisynthetic glycopeptide antibiotics: the guanidino lipoglycopeptides (for chemical structures see **Chapter 2 Fig. 2**). The guanidino lipoglycopeptides contain a unique structural modification not found in any clinically used glycopeptides, consisting of a guanidino moiety (positively charged at physiological pH) connected to various aliphatic and aromatic groups. These novel glycopeptides exhibit enhanced *in vitro* activity against a panel of clinically relevant Gram-positive bacteria including clinically relevant MRSA, vancomycin-resistant strains, and *Clostridia*.

Importantly, here we report that the potent *in vitro* antibacterial activity against Gram-positive bacteria is also mirrored by the *in vivo* efficacy demonstrated for the guanidino lipoglycopeptides in murine thigh infection and sepsis survival models. In addition, the guanidino lipoglycopeptides exhibit promising PK properties, are non-toxic to eukaryotic cells, and demonstrate a low propensity to select for resistance. Detailed mechanistic studies reveal that the guanidino lipoglycopeptides bind to the bacterial cell wall precursor lipid II with a much higher binding affinity than vancomycin. Notably, tight binding to both wild-type lipid II and the vancomycin-resistant variant was confirmed, providing key insight into the enhanced activity of the guanidino lipoglycopeptides against vancomycin-resistant isolates. In this light, the guanidino

lipoglycopeptides represent a promising new class of semisynthetic glycopeptides for the treatment of Gram-positive infections.

3.2 Results and Discussion

3.2.1 *In vitro* assessment of the guanidino lipoglycopeptides in cell-based assays

It is known that the activity of compounds containing large hydrophobic groups can be impacted by nonspecific interactions with serum proteins.[10,11] For this reason, we examined the antibiotic activity of the guanidino lipoglycopeptides in the presence of 50% sheep serum (**Table 1**). While the clinically used lipoglycopeptides **2-5** all have a 4-8-fold reduction in activity in the presence of serum, the same is not observed for the guanidino lipoglycopeptides. For compounds **6-7, 10-11, 13-14, 16,** and **18** only minimal changes in antibacterial activity are observed upon addition of serum to the media. Among the remaining guanidino lipoglycopeptides, addition of serum does impact activity although not in a manner indicating a specific trend: while compounds **8** and **9**, bearing linear C_8 and C_9 substituents respectively, do show an 8-fold reduction in activity in the presence of serum, the MIC values of compounds **10** and **11,** bearing linear C_{10} and C_{11} lipids, are only increased by a factor of two. For analogues **16-20**, containing a variety of structurally diverse substituents, the farnesylated compound **17** experiences a large 16-fold reduction of activity in the presence of serum, while compounds **16** and **18-20** experience only 2-4 fold increases in MIC.

In parallel to studying the impact of serum proteins on the activity of the guanidino lipoglycopeptides, we also assessed the capacity for the guanidino lipoglycopeptides to lyse erythrocytes (**Fig. 1**). Such hemolysis assays provide a convenient mean to assess whether a compound displays general membrane disruptive properties. Most of the guanidino lipoglycopeptides exhibit very minimal hemolytic activity when tested up to 1,000-fold MIC (MIC values based on activity against MRSA). Especially those derivatives with smaller substituents (**6-9**, **13**, **14**, **16**, **18-20**) induce only marginal hemolysis at the highest concentrations tested, whereas the clinically used oritavancin causes 50% hemolysis when tested at the 1000xMIC concentration. Notably, the guanidino lipoglycopeptides containing the largest hydrophobic groups are significantly hemolytic. Compounds **10** and **17** cause hemolysis similar to oritavancin when tested at 1000xMIC, while compounds **11**, **12**, and **15** exhibit significant hemolytic activity at 100xMIC. Building upon the findings of the MIC and hemolysis assays, compounds **7**, **14**, and **18** were taken forward for additional cytotoxicity screening with HepG2 and HEK293T cells. These assays revealed that compound **7** is not cytotoxic up to the highest concentration tested (100 μM), even while using only 1% Fetal Bovine Serum (FBS) to ensure low plasma protein binding and therefore high compound

availability. In contrast, compounds **14** and **18** are more toxic with CC_{50} values comparable to the clinically used lipoglycopeptides telavancin and oritavancin respectively (**Table 2**).

Table 1. MIC of the guanidino lipoglycopeptides against MRSA USA300 with and without 50% serum

MIC (µg/mL)				Fold increase in MIC
Compound		Conditions		
Id	**Structure**	**MRSA[a]**	**+ 50% serum[b]**	
1	Vancomycin	1	0.25	0.25
2	Teicoplanin	0.5	2	4
3	Telavancin	0.125	1	8
4	Dalbavancin	0.25	2	8
5	Oritavancin	0.063	0.25	4
Guanidino lipoglycopeptides				
6	$-C_6H_{13}$	0.063	0.063	1
7	$-C_7H_{15}$	0.016	0.031	2
8	$-C_8H_{17}$	≤0.008	0.063	≥8
9	$-C_9H_{19}$	≤0.008	0.063	≥8
10	$-C_{10}H_{21}$	0.063	0.125	2
11	$-C_{12}H_{25}$	0.5	1	2
12	$-C_{14}H_{29}$	4	16	4
13	$-C_4H_9$ $-C_4H_9$	0.125	0.063	0.5
14	$-C_6H_{13}$ $-C_6H_{13}$	0.063	0.063	1
15	$-C_{10}H_{21}$ $-C_{10}H_{21}$	16	64	4
16[c]	-Ger	0.031	0.063	2
17[d]	-Far	0.063	1	16
18[e]	$-CH_2$-CBP	0.031	0.063	2
19[f]	-TCD	0.031	0.125	4
20[f]	$-CH_2$-TCD	≤0.008	0.031	≥4

MIC values are the median of a minimum of triplicates. MIC = minimum inhibitory concentration. [a]Methicillin-resistant S. aureus USA300. [b]Methicillin-resistant S. aureus USA300 + 50% sheep serum. [c]Ger = geranyl. [d]Far = farnesyl. [e]CBP = 4-chloro-1,1'-biphenyl. [f]TCD = tricyclo[3.3.1.13,7]decane or adamantane

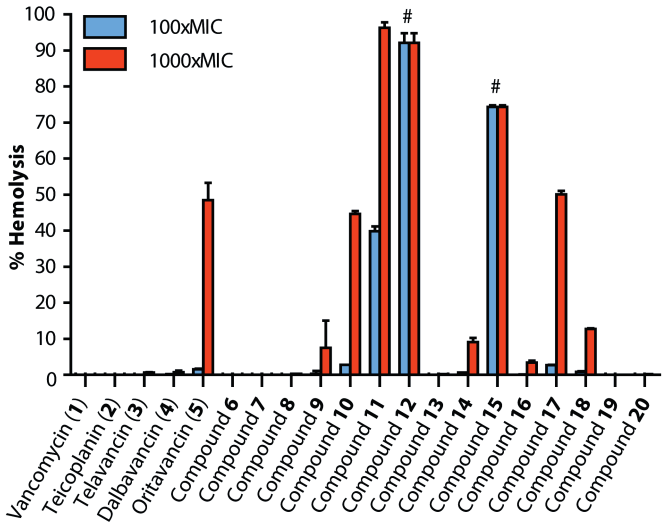

Fig. 1. Hemolysis analysis of the guanidino lipoglycopeptides. Percent hemolysis of compounds **1-20** at 100- and 1,000-fold MIC (based on MRSA USA 300) against sheep erythrocytes after 18 h incubation. Data were normalized by subtraction of the signal derived from the buffer and compared with a completely lysed sample treated with Triton X-100. Data are mean ± SD of a minimum of triplicates. At 1,000-fold MIC, DMSO stocks of **12** and **15** were insoluble and therefore not measured: the % hemolysis can be expected to be higher than the value at 100-fold MIC for these compounds, therefore the values of 100-fold MIC are plotted here (#). MIC = minimum inhibitory concentration.

Table 2. Mammalian cytotoxicity of the guanidino lipoglycopeptides.

	Cytotoxicity CC_{50} (µM)	
Structure	**HepG2**	**HEK293T**
Vancomycin (**1**)	>50	>50
Telavancin (**3**)	>50	24
Oritavancin (**5**)	9.0	3.5
Compound **7**	>100	>100
Compound **14**	63	27
Compound **18**	14	5.3

CC_{50} (µM) after 24 h as measured by MTT assay in HepG2 and HEK293T cells grown in the presence of 1% FBS (biological replicates n = 2). *Experiment performed by Alexander Bakker.*

We next examined the time-kill kinetics of the guanidino lipoglycopeptides in comparison to the clinically used vancomycin, telavancin, and daptomycin. These studies revealed the guanidino lipoglycopeptides to have a slow bactericidal effect against VRE and MRSA, similar to the glycopeptides vancomycin and telavancin (**Fig. 2**). The time-kill data also confirm the previous results of the broth microdilution assays which show that significantly lower concentrations of the guanidino lipoglycopeptides are required

compared to clinically used glycopeptide antibiotics to achieve the same reduction in bacterial titer. In addition, superior activity is evident for compound **7** when compared to daptomycin, which is clinically used in the treatment of MRSA infections. While administration of daptomycin (at 5 µg/mL) leads to an initial quick drop in colony forming units (CFUs) for MRSA, after 24 hours a high bacterial titer is again present. By comparison, when the more potent guanidino lipoglycopeptide **7** is used (at 0.156 µg/mL) no colonies are detected at 24 hours (**Fig. 2B**).

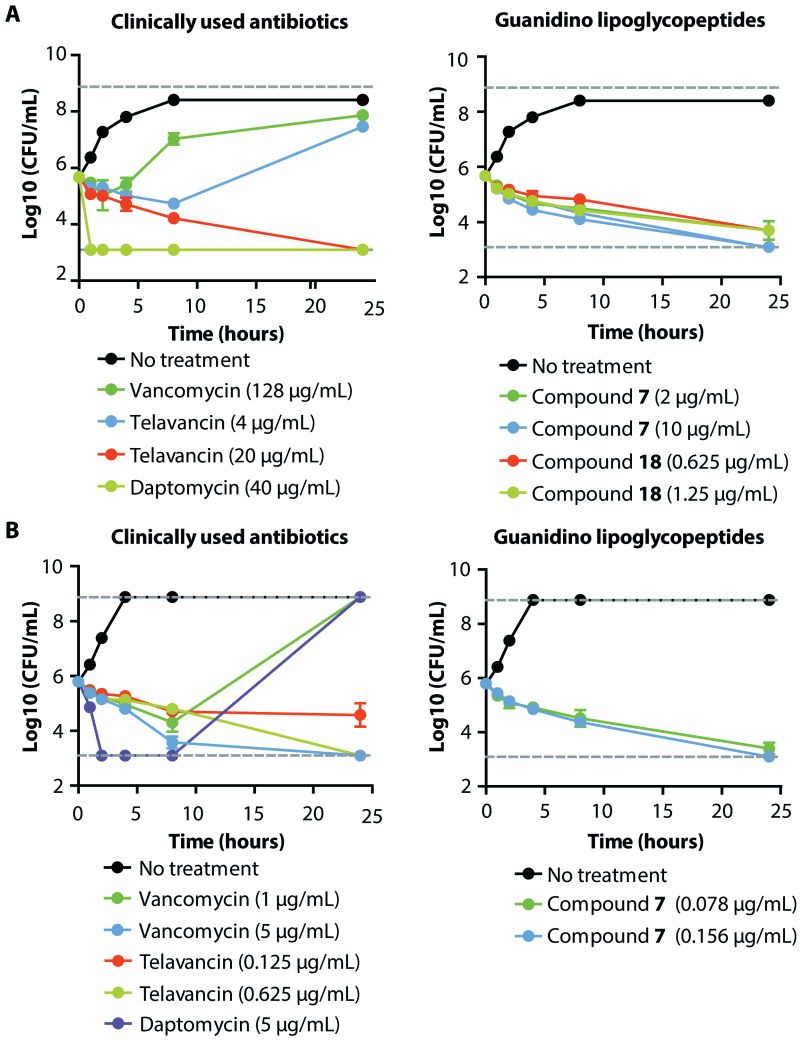

Fig. 2. Time-kill kinetics of the guanidino lipoglycopeptides. Bactericidal activity of vancomycin, telavancin, daptomycin (left) and compound **7** and **18** (right) against (**A**) VRE-E155 and (**B**) MRSA US300 as measured by agar plate dilution colony count of samples at different time intervals. Gray dotted lines represent limits of detection. Experiments performed in biological replicates (n=2) plated out in technical duplicates. CFU = colony forming units.

We also investigated the propensity for the guanidino lipoglycopeptides to select for resistance. When a VanA-type VRE strain is serially passaged over 30 days in the presence of sub-lethal antibiotic concentrations, compounds **7** and **18**, bearing C_7 or chlorobiphenyl lipids respectively, only display limited resistance selection (**Fig. 3A**). By comparison, under the same conditions and using the same bacterial strain, a significant level of resistance is selected against the clinically used daptomycin with a 128-fold increase in MIC. Similar findings are also made when using an MRSA strain: again, low-level resistance is observed for compound **7** and **18** while resistance to daptomycin rapidly develops (**Fig. 3B**).

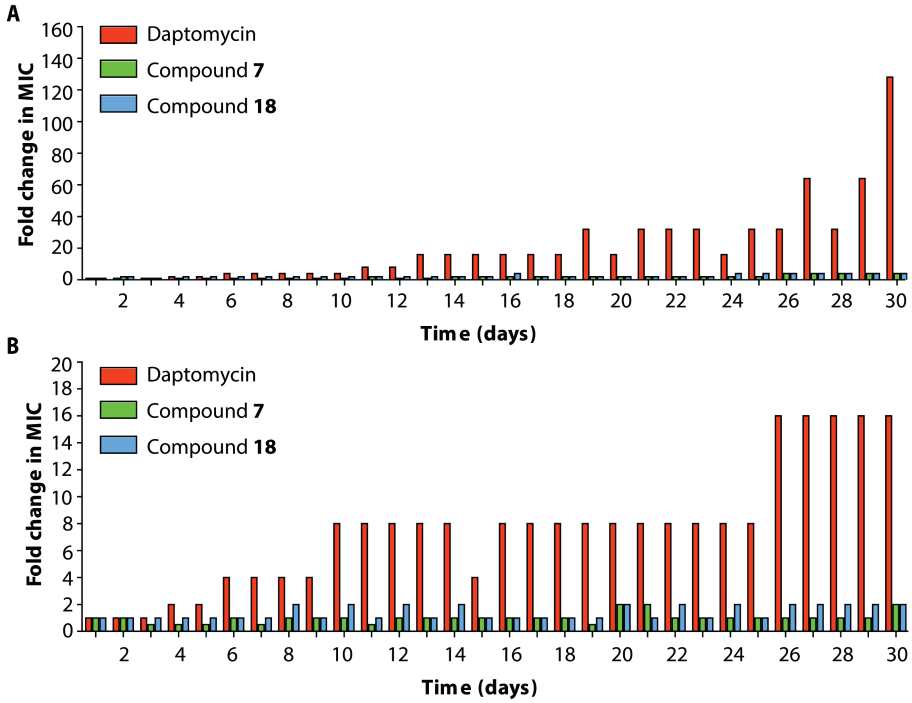

Fig. 3. Selection for resistance to guanidino lipoglycopeptides. Daily fold-increase of MIC against (**A**) VRE-E155 and (**B**) MRSA USA300 grown in sub-lethal concentrations of daptomycin, compound **7** or compound **18** over 30 days. Experiments were performed in biological replicates (n=2) in technical triplicates. Data are shown as median of triplicates of one biological replicate, and is representative for both biological replicate experiments. Resistance selection to vancomycin was absent for MRSA, giving similar graphs as **7** and **18** (data not shown). MIC = minimum inhibitory concentration.

After establishing the low propensity of the guanidino lipoglycopeptides to select for resistance, we investigated their anti-biofilm activity. Biofilm formation is an increasingly recognized clinical challenge in the treatment of bacterial infections, wherein bacteria form a protective layer capable of blocking antibiotic and immune system activity.[12] The biofilm matrix usually adheres to important human tissues, such as heart

valves and bones, or to implanted medical devices such as pacemakers and catheters.[12] As biofilm forming pathogens are often MDR,[13] the development of novel and effective anti-biofilm treatments is essential. Persistent infections in patients are largely caused by pathogens that are strong biofilm producers, with *S. aureus* being one of the main culprits.[13,14] Therefore, we determined the minimal biofilm inhibitory concentration (MBIC) and minimal biofilm eradication concentration (MBEC) against *S. aureus* ATCC25923, a strain reported to form strong biofilms[15] (**Table 3, Fig. S1, Fig. S2**). Notably, compound **7** has an 8- and 16-fold lower MBIC compared to dalbavancin and oritavancin respectively. Compound **7** is also a potent biofilm eradicator, with a MBEC of 2 µg/mL, representing a 2- and 8-fold improved value compared to dalbavancin and oritavancin respectively. Given its potent antibacterial and anti-biofilm activity, coupled with its minimal propensity for resistance selection and low toxicity in cell-based assays, compound **7**, in which the guanidino moiety is substituted with the linear C_7 lipid, was prioritized for the subsequent mechanistic and *in vivo* studies.

Table 3. MIC, MBIC and MBEC values against *S. aureus* ATCC25923.

	Compound 7	Dalbavancin	Oritavancin
MIC (µg/mL)	0.004	0.008	0.125
MBIC (µg/mL)	0.0625	0.5	1
MBEC (µg/mL)	2	4	16

Strain was treated with compound **7,** dalbavancin and oritavancin. For determination of MBICs antibiotics were added with the inoculum before biofilm formation. MBECs were determined by addition of compounds to preformed biofilm. MICs were determined by standard broth microdilution. MBIC and MBEC were detected using the Innovotech peg lid system. *Experiment performed by Melina Arts/Stefania De Benedetti.*

3.2.2 Mechanistic studies with the guanidino lipoglycopeptides

Our mechanistic investigations of the guanidino lipoglycopeptides began by examining their capacity to impact the bacterial cell wall. It is well established that vancomycin interferes with late-stage cell wall biosynthesis.[16] This effect can be studied by measuring the accumulation of UDP-MurNAc-pentapeptide (the final soluble precursor in the bacterial cell wall synthesis cycle) that occurs upon treatment with cell wall active antibiotics such as the glycopeptides.[16–18] Our work clearly shows that treatment of *S. aureus* with the guanidino lipoglycopeptides also leads to UDP-MurNAc-pentapeptide accumulation, thus confirming that they inhibit cell wall biosynthesis (**Fig. 4**). To obtain a more global view of the impact the guanidino lipoglycopeptides have on bacterial morphology, light microscopy was used to image the model species *B. subtilis* in response to antibiotic treatment. Visualization of bacterial cells treated with vancomycin, oritavancin, or compound **7** at 5xMIC reveals similarly significant cell deformations with disintegration of the peptidoglycan layer inducing formation of membrane blebs (**Fig. 5**).

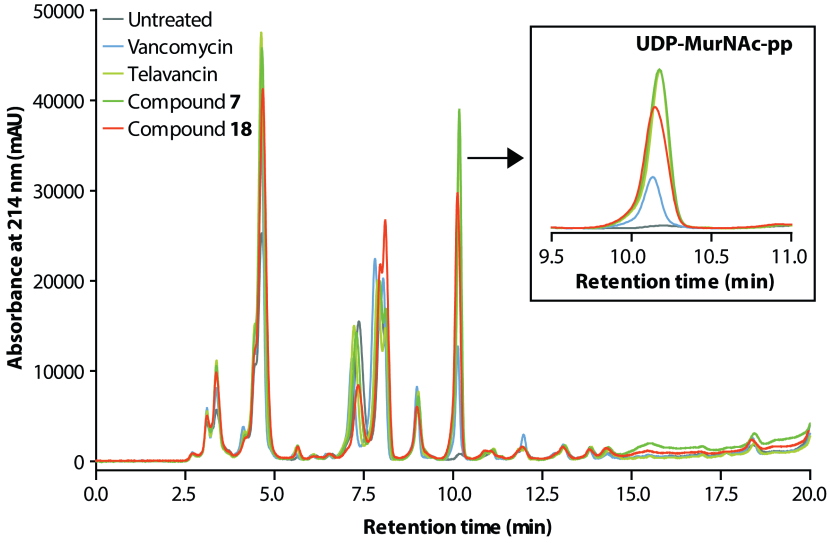

Fig. 4. UDP-MurNAc-pentapeptide accumulation assay. HPLC-based accumulation assay of intracellular cell wall precursor UDP-*N*-acetylmuramyl-pentapeptide (UDP-MurNAc-pp) in *S. aureus* ATCC29213. Vancomycin, teicoplanin, telavancin, dalbavancin, oritavancin, compound **7**, and compound **18** all accumulate the last soluble precursor of the peptidoglycan layer UDP-MurNAc-pp. Negative control (untreated) shows no accumulation.

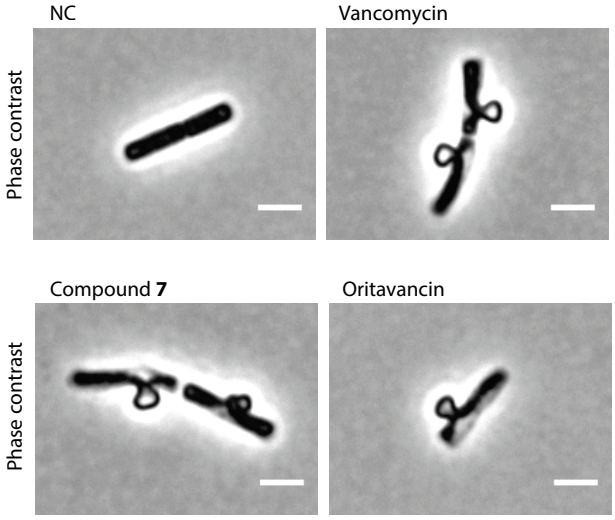

Fig. 5. Microscopic analysis of *B. subtilis* membrane blebbing by antibiotics. Compound **7** causes major cell deformations and disruption of the cell wall leading to formation of membrane blebs. Deformations were detected for vancomycin and oritavancin as controls. Antibiotics were tested at 5xMIC and incubation time was 30 min. Scale bar represents 2 µm. Pictures are representative for biological triplicates. *Experiment performed by Melina Arts/Stefania De Benedetti.*

The manner in which vancomycin inhibits cell wall biosynthesis involves sequestration of the cell wall precursor lipid II.[2,3,5,19] A well-defined network of hydrogen bond interactions enables vancomycin to specifically bind to the D-Ala-D-Ala terminus of the lipid II pentapeptide which in turn prevents cell wall crosslinking.[2–5] The binding affinity of vancomycin to lipid II is enhanced by cooperative dimerization.[20,21] We confirmed that the guanidino lipoglycopeptides retain this lipid II-D-Ala (LII-D-Ala) dependent mechanism of action by means of a lipid II antagonization assay. In doing so, addition of exogenous LII-D-Ala was shown to effectively antagonize the activity of the compounds at 8xMIC indicating strong lipid II binding (**Table S1**). To gain deeper insights into the lipid II binding capacity of the guanidino lipoglycopeptides, we now employed isothermal titration calorimetry (ITC) wherein large unilateral vesicles (LUVs) comprised of dioleoylphosphatidylcholine (DOPC) containing LII-D-Ala were titrated into solutions of vancomycin or compound **7**. Control titrations of buffer into the sample cell containing solutions of the antibiotics reveal no binding (**Fig. S3** and **S4**) nor does titration of blank LUVs into the antibiotics (**Fig. S5** and **S6**). Titration of LII-D-Ala containing vesicles into vancomycin provides a well-defined thermogram with an associated dissociation constant (K_D) of 1170 nM (**Fig. 6A**). By comparison, when the same binding study is performed with guanidino lipoglycopeptide **7**, a K_D value nearly 10-fold lower (120 nM) is measured, indicative of a tighter binding interaction between the antibiotic and LII-D-Ala (**Fig. 6B**). Further insights into the capacity for compound **7** to maintain its potent antibacterial activity against vancomycin-resistant strains were obtained by performing binding studies with the D-Ala-D-Lac form of lipid II (LII-D-Lac). Mutation of the D-Ala-D-Ala terminus of the lipid II pentapeptide to D-Ala-D-Lac is known to significantly impact the antibacterial activity of vancomycin.[6,7] In accordance with this, our ITC studies with LUVs containing LII-D-Lac reveal a total loss of vancomycin binding, with no measurable interaction detected (**Fig. S9**). In contrast, when LUVs containing LII-D-Lac are titrated into a solution of compound **7**, a clear indication of binding is observed with a measured K_D value of 813 nM (**Fig. 6C**). While this indicates a nearly 7-fold reduction in binding affinity relative to the wild type LII-D-Ala, it is notable that in absolute terms, compound **7** exhibits a higher binding affinity for the mutant LII-D-Lac than vancomycin does for native LII-D-Ala (see **Table S2** for full thermodynamic parameters and **Fig. S7–10** for all triplicate titrations).

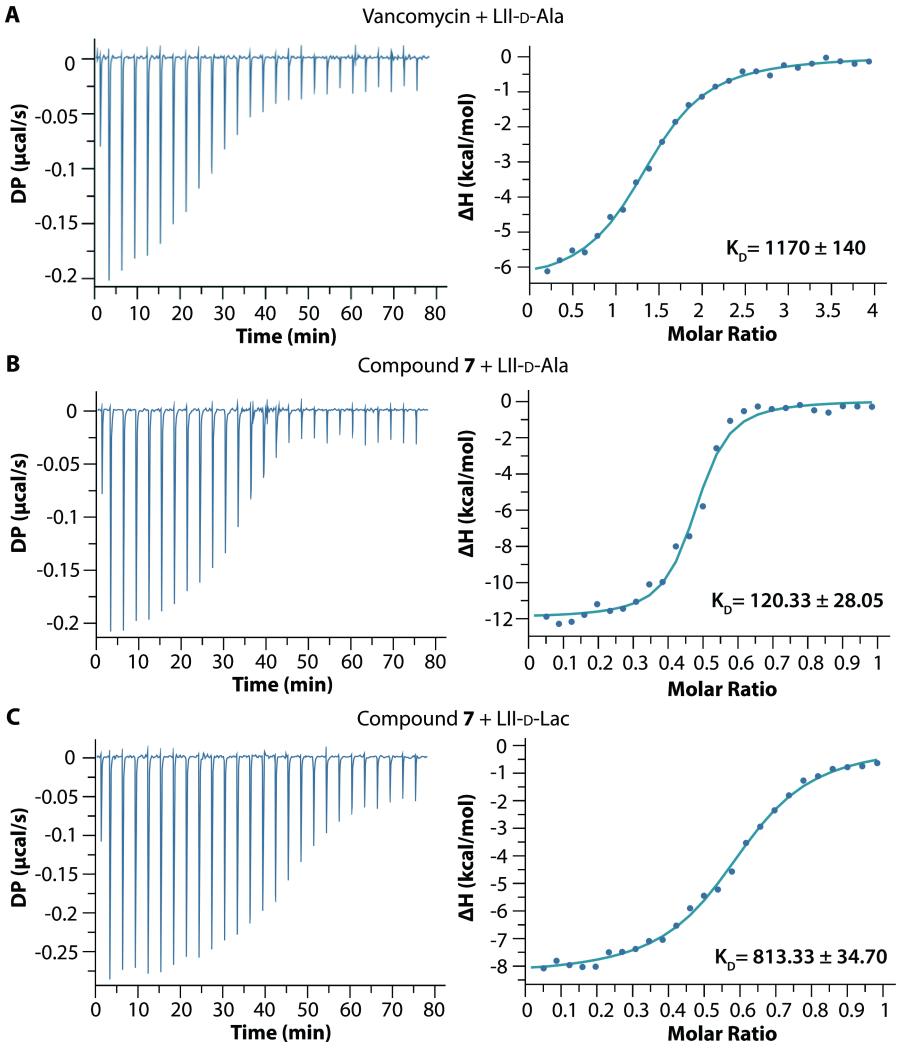

Fig. 6. Lipid II binding of the guanidino lipoglycopeptides assessed by ITC. (**A**) Representative binding isotherms for the titrations of 200 µM LII-D-Ala, 10 mM DOPC LUVs to vancomycin (10 µM), (**B**) 100 µM LII-D-Ala, 10 mM DOPC LUVs to compound **7** (20 µM), and (**C**) 200 µM LII-D-Lac, 10 mM DOPC LUVs to compound **7** (20 µM). Titrations performed in triplicates (n=3). A single titration (n=1) is displayed and is representative for all triplicates. See **Table S2** for full thermodynamic parameters and **Fig. S7-10** for all triplicate titrations. *Experiment performed by Ioli Kotsogianni.*

To further investigate the impact of the guanidino lipoglycopeptides on cell wall synthesis and lipid II binding, induction of cell wall stress responses upon treatment with compound **7** were studied using a luminescence-based assay.[22–24] These studies revealed that the *S. aureus* VraRS-lux and *B. subtilis* LiaI-lux bioreporters are both activated in response to increasing concentrations of compound **7** (**Fig. 7, Fig. S11**). These stress

responses are known to be upregulated upon treatment with cell wall active antibiotics.[22] Notably, the induction of *B. subtilis* stress response is fully antagonized by addition of wild type lipid I and LII-D-Ala at a 2:1 lipid:compound ratio for compound **7**, **14**, and **18** as well as for vancomycin and oritavancin (**Fig. 7A**, **Fig. S12**). Furthermore, the addition of LII-D-Lac, albeit at higher concentrations, also antagonizes the stress response induced by guanidino lipoglycopeptides, further substantiating that the guanidino lipoglycopeptides bind to both native D-Ala and mutant D-Lac forms of lipid II. Full antagonization with LII-D-Lac is achieved at a 8:1 lipid:compound **7** ratio, similar to oritavancin (also known to interact with LII-D-Lac)[25] (**Fig. 7BC**). By comparison and in line with expectations, little antagonization of the cell wall stress response induced by vancomycin in *B. subtilis* is observed upon addition of LII-D-Lac (**Fig. 7A**). To further confirm the D-Ala-D-Ala motif as the primary target of the guanidino lipoglycopeptides, we also included the lipid I/II phospholipid carrier undecaprenyl pyrophosphate (C_{55}PP) in the antagonization studies (**Fig. S12**). This showed that C_{55}PP does not antagonize the LiaI-lux response and thus does not seem to be a relevant target of the guanidino lipoglycopeptide antibiotics.

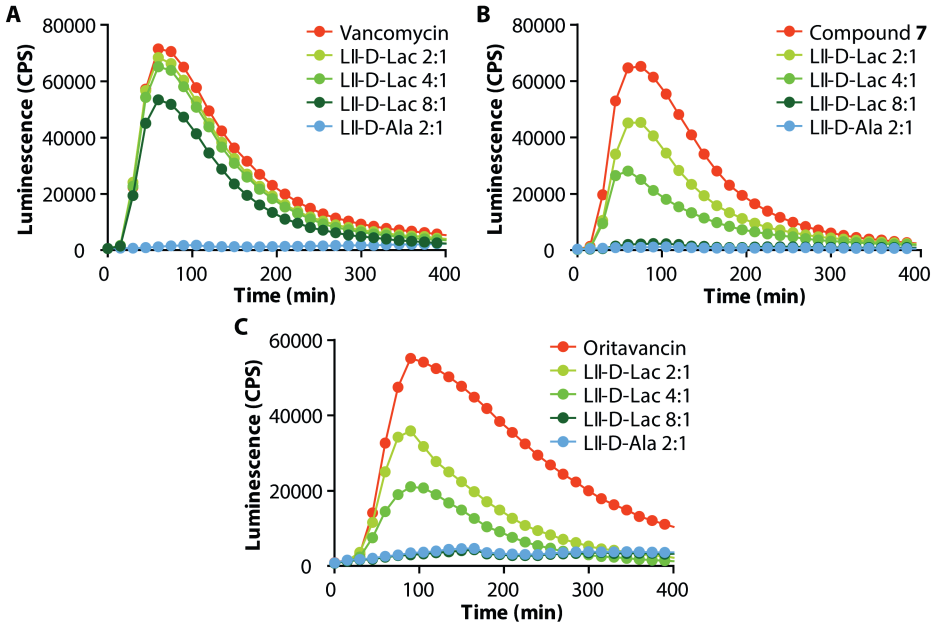

Fig. 7. Induction and antagonization of cell-wall stress responses. Induction of cell wall stress response by (**A**) vancomycin, (**B**) compound **7**, (**C**) and oritavancin in *B. subtilis* reporter strains and antagonization by LII-D-Ala and -D-Lac. Graph representative of n=2. *Experiment performed by Melina Arts/Stefania De Benedetti.*

The capacity for the guanidino lipoglycopeptides to form stable complexes with either the native LII-D-Ala or the LII-D-Lac form was next assessed. Compounds **7**, **14**, and **18** form extraction-stable complexes with LII-D-Ala at a 2:1 molar ratio (glycopeptide:LII) (**Fig. S13**), indicating potential dimerization, a phenomenon not uncommon for glycopeptide antibiotics.[21,26] In contrast, the guanidino lipoglycopeptides do not form extraction-stable complexes with LII-D-Lac, nor do vancomycin or oritavancin. We also examined the ability of compound **7** to block various enzymatic processes associated with cell wall synthesis when using LII-D-Lac as substrate. These studies revealed that compound **7** exhibits a dose-dependent inhibition of reactions catalyzed by: 1) MurT/GatD, which normally amidates lipid II at the Glu residue of the stem peptide, and 2) PBP2, which catalyzes lipid II transglycosylation. In general, full inhibition of both enzymatic processes was observed at a 10-fold excess of compound **7** (**Fig. 8**). By comparison, the PBP2 mediated transglycosylation reaction with native LII-D-Ala is nearly fully inhibited at an equimolar ratio of **7**, indicating a stronger binding interaction (**Fig. 8C**).

Given that lipoglycopeptides can exhibit membrane targeting properties,[4,20,27–29] we next turned to the use of membrane-selective fluorescent dyes to determine whether the guanidino lipoglycopeptides also cause membrane disruption. In the first instance, we used dipropylthiadicarbocyanine iodide ($diSC_3(5)$), a probe that resides on hyperpolarized membranes and is released upon disruption of the membrane potential.[30] These studies showed that no membrane depolarization is induced by the guanidino lipoglycopeptides when applied at a concentration of 1.5 µg/mL, while the known membrane disrupting and lipid II targeting lantibiotic nisin clearly causes membrane depolarization at the same concentration (**Fig. 9A, Fig. S14**). In general, compound **7** shows little effect on membrane polarization, even at the highest concentration tested of 16 µg/mL. By comparison, when the clinically used oritavancin is also tested at 16 µg/mL, it is found to dissipate membrane potential (**Fig. S14**), a finding in keeping with previous reports.[31,32] Membrane perturbation effects were also examined by use of propidium iodide (PI), a DNA-binding dye that can enter cells and fluoresce after pore formation.[33] In this assay, compound **7** is again found to be less membrane disruptive relative to oritavancin (**Fig. 9B, Fig. S15**) which is known to induce PI fluorescence in bacterial cells.[32] We next investigated the impact of the guanidino lipoglycopeptides on the cell division regulator MinD in *B. subtilis*. The activity of MinD is modulated by the membrane potential and it has previously been shown that under normal conditions a GFP-MinD construct localizes to the septum and cell poles. However, once the membrane potential is dissipated, it rapidly delocalizes.[34] The lipid II dependent membrane disruptor nisin causes dissipation of the membrane potential, which in turn is visible as a spotty pattern associated with the GFP-MinD construct in the fluorescent microscopy read out. Contrary to nisin, compound **7** and oritavancin do not induce delocalization of membrane-potential driven GFP-MinD

in early exponential phase cultures of *B. subtilis* (**Fig. 10**). The absence of membrane permeabilization or depolarization is typically seen as favorable, given that antibacterial agents that function via membrane disruption are often linked to perturbation of mammalian cell membranes leading to off-target effects and toxicity.[29,35]

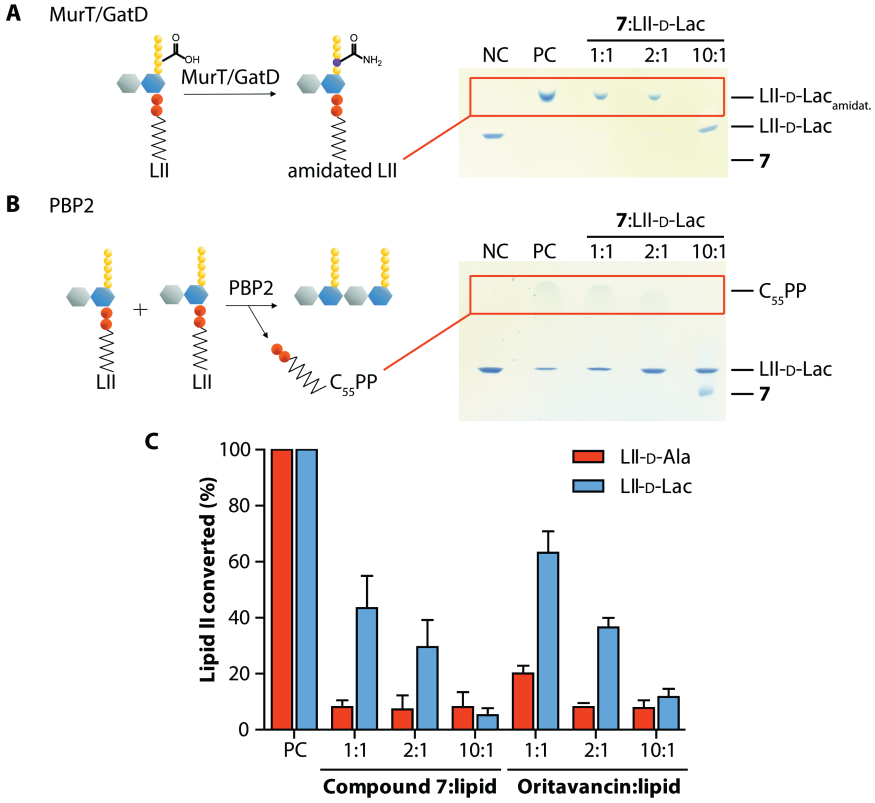

Fig. 8. Inhibition of enzyme catalyzed reactions on lipid II. (**A**) Amidation of LII at the Glu residue of the stem peptide is catalyzed by the MurT/GatD enzyme complex. TLC analysis of MurT/GatD catalyzed reactions *in vitro* using LII-D-Lac as substrate. Decreased formation of amidated LII-D-Lac (orange box) indicates MurT/GatD inhibition. Visualized by TLC – TLC is representative of three independent experiments. (**B**) PBP2 catalyzed LII transglycosylation resulting in polymerized PGN and release of C_{55}-PP. TLC analysis of PBP2 catalyzed reactions *in vitro* using LII-D-Lac as substrate. Decreased release of C_{55}-PP (orange box) indicates PBP2 inhibition. Visualized by TLC – TLC is representative of three independent experiments. (**C**) Impact of compound **7** on the PBP2-catalyzed transglycosylation reaction using LII-D-Ala (orange) and LII-D-Lac (blue) as substrates. Enzymatic activity is expressed as converted LII. The control reactions in the absence of antibiotics were set to 100%. Data are mean ± SD (n=3). *Experiment performed by Melina Arts/Stefania De Benedetti.*

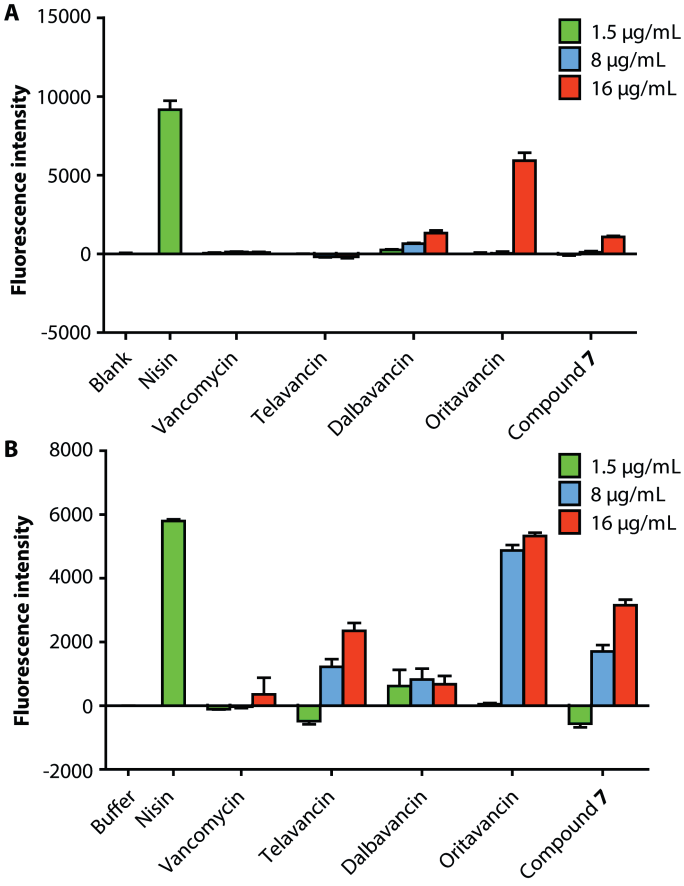

Fig. 9. Membrane depolarization and pore formation assessment of the guanidino lipoglycopeptides. (**A**) Membrane depolarization assessment of vancomycin, telavancin, dalbavancin, oritavancin, and compound **7** at 1.5 µg/mL, 8 µg/mL, and 16 µg/mL after 20 min using $diSC_3(5)$ against MRSA USA300. Fluorescence intensity of $diSC_3(5)$ releasing from the membrane of MRSA USA300 in the presence of antibiotic. $diSC_3(5)$ is a cationic fluorescent probe that accumulates on hyperpolarized membranes and translocates to the lipid bilayer. Upon disruption of the membrane potential $diSC_3(5)$ can no longer partition to the cell surface, resulting in release of the dye into the media, which can be measured by an increase in fluorescence. After 3 minutes of incubating $diSC_3(5)$ and bacterial cells, compounds were added, and a 30-minute time course was recorded. All data were normalized by subtraction of the signal derived from the buffer. Nisin at 1.5 µg/mL was used as positive control. Data are mean ± SD (n=3). (**B**) Pore formation assessment of vancomycin, telavancin, dalbavancin, oritavancin, and compound **7** at 1.5 µg/mL, 8 µg/mL, and 16 µg/mL after 20 min using propidium iodide dye against MRSA USA300. Fluorescence intensity of propidium iodide (PI) binding to DNA of MRSA USA300 in the presence of antibiotics was recorded in a 30-minute time course. PI is a red-fluorescent dye impermeable to live cells. Upon pore formation PI enters cells and binds DNA resulting in an increased fluorescence signal. All data were normalized by subtraction of the signal derived from the buffer. Nisin at 1.5 µg/mL was used as positive control. Data are mean ± SD (n=3).

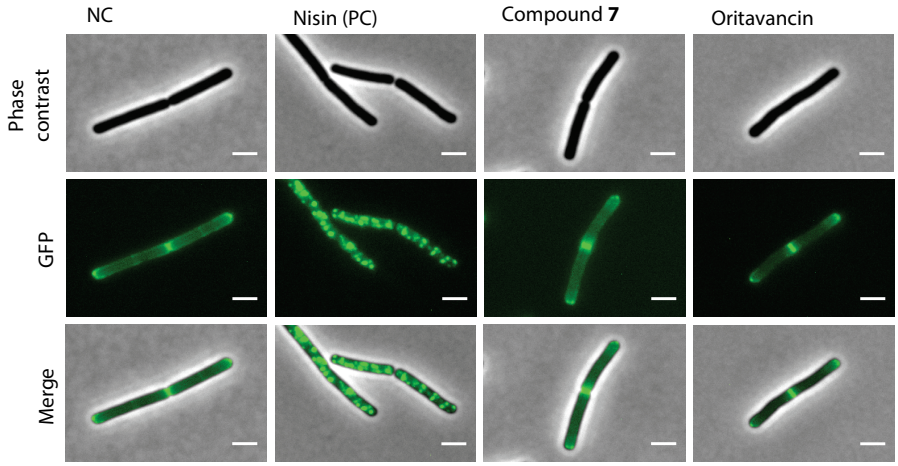

Fig. 10. Microscopic analysis of the membrane potential-dependent localization pattern of MinD in *B. subtilis*. In untreated cells GFP-MinD localizes to the septum and cell poles. Comparable to oritavancin, compound **7** treatment does not lead to GFP-MinD delocalization after 15 min. Nisin was used as a positive control showing GFP-MinD delocalization (spotty pattern). Scale bar represents 2 µm. Pictures representative of biological triplicates. *Experiment performed by Melina Arts/Stefania De Benedetti.*

3.2.3 *In vivo* studies

The outstanding performance of compound **7** in the mechanistic and *in vitro* cell-based assays described above led to its further evaluation in a number of *in vivo* models. Initial tolerability studies in mice revealed compound **7** to be well tolerated at doses up to 100 mg/kg via subcutaneous (SC) administration and 50 mg/kg via intravenous (IV) administration. Notably, when dosed at 3 mg/kg SC, pharmacokinetic analysis indicates that compound **7** has a half-life of 1.22 hours and maintains bloodstream concentrations >MIC (based on activity against MRSA USA300) for >8 hours indicating good exposure (**Fig. 11, Table S3**).

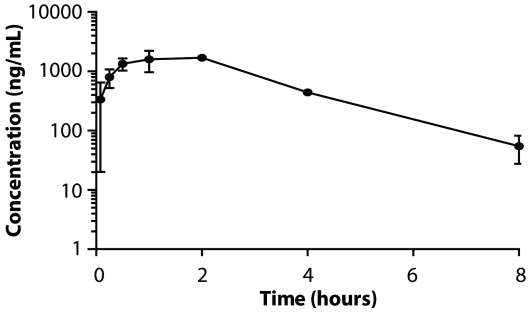

Fig. 11. Mouse PK of guanidino lipoglycopeptide 7. Pharmacokinetic profile of blood concentrations of compound **7**. Compound **7** was administered subcutaneous at 3 mg/kg in mice, followed by serial sampling. Data are mean ± SD (n=3).

Subsequently, *in vivo* efficacy was assessed using an established MRSA murine thigh infection model.[36] Immunosuppressed mice were infected with MRSA and subsequently treated with vehicle, compound **7** (3 mg/kg or 10 mg/kg, SC, dosing interval q6h), or vancomycin (25 mg/kg, IV, q12h) as a clinical reference antibiotic (**Fig. 12**). Notably, the lowest dose evaluated for compound **7** (3 mg/kg, SC, q6h, total cumulative dose 12 mg/kg) results in a near 6-log reduction in bacterial titer compared to the vehicle treatment group. This response compares very well to that seen in the vancomycin group, which was treated with a much higher dose (25 mg/kg, IV, q12h, total cumulative dose 50 mg/kg). Furthermore, when the dosing of compound **7** is increased to 10 mg/kg (SC, q6h, total cumulative dose 40 mg/kg) an even greater reduction in bacterial load is achieved corresponding to a 7-log reduction compared to vehicle. Overall, compound **7** displays a clear dose-dependent effect and is bactericidal at all tested doses reducing bacterial burden significantly to below pretreatment levels (**Fig. 12**, see **Table S4** and **S5** for individual data and statistical analysis). Importantly, these findings also mirror the result of the MIC assays (**Chapter 2**), clearly demonstrating that the activity of compound **7** is not only superior to that of vancomycin *in vitro* but also in the more complex *in vivo* setting.

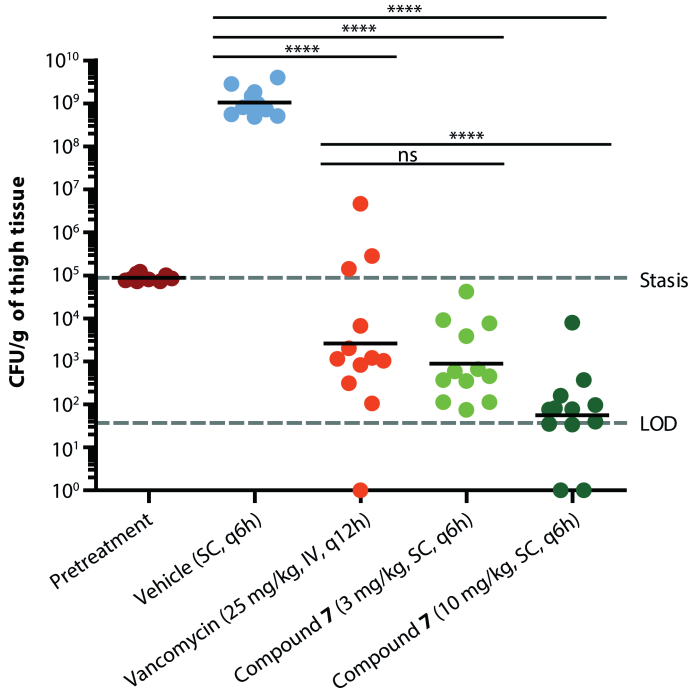

Fig. 12. *In vivo* efficacy of guanidino lipoglycopeptide 7 in a murine thigh infection model. Colony forming units measured in thigh muscle tissue of neutropenic mice infected in each thigh with MRSA USA300 followed by antibiotic treatment at concentrations and dose intervals indicated. 23 h post infection the mice were sacrificed and bacterial load determined. Bar = geometric mean (n=12, six mice per group, two thighs per mouse). LOD = Limit of detection. q indicates dosing interval. ****p≤0.0001.

The capacity for the guanidino lipoglycopeptides to treat systemic infection *in vivo* was next investigated in a 7-day sepsis survival study. To do so, a sepsis model was used wherein immunocompetent mice were infected IV with *S. aureus* NCTC8178. One hour post infection, treatment commenced with compound **7** over a 24-hour period, dosed at different treatment regimens, vancomycin (25 mg/kg, IV, q12h), or vehicle after which survival was monitored for a total of 169 hours (**Fig. 13**). The mice receiving vehicle only survived 51.3 hours on average while the vancomycin-treated mice had a mean survival of 131.5 hours with only one out of ten mice surviving to the end of day 7. In contrast, in the group treated with compound **7**, dosed according to the same regimen used in the vancomycin group (25 mg/kg, IV, q12h, total cumulative dose 50 mg/kg), all mice survived to the end of the study (≥169 hours survival). Also of note was the finding that when administered at lower doses, compound **7** still significantly outperforms vancomycin. In the groups treated with compound **7** at 10 mg/kg (SC, q6h, total cumulative dose 40 mg/kg) or 3 mg/kg (SC, q6h, total cumulative dose 12 mg/kg) 10/10 mice and 9/10 mice respectively survived to the 7-day endpoint (see **Table S6**, **S7** and **S8** for individual data and statistical analysis).

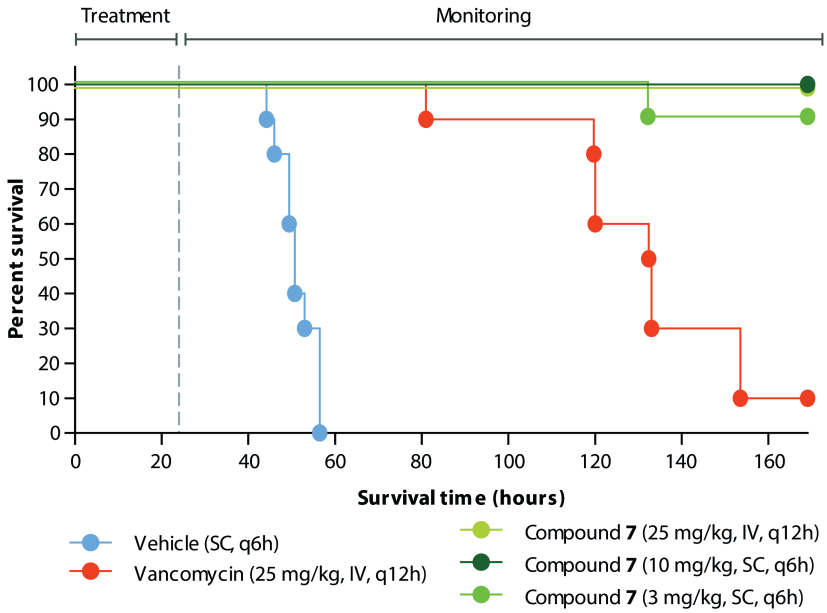

Fig. 13. *In vivo* efficacy of guanidino lipoglycopeptide 7 in a murine sepsis survival study.
Kaplan Meier plot of survival following infection with *S. aureus* NCTC8178 in healthy mice. Starting 1 h post-infection immunocompetent mice were treated for 24 h (until the vertical dotted bar) and monitored for a total of 169 h (7 days). Each group consisted of n=10 mice. q indicates dosing interval.

Building upon these promising findings we also examined the organ-specific effect of compound **7** in reducing *S. aureus* NCTC8178 bacterial burden. This involved a sepsis model wherein immunocompetent mice were IV infected with *S. aureus* after which they were treated with either vehicle or antibiotic for 24 hours and monitored for an additional 25 hours. The animals were then sacrificed and the bacterial burden in the spleen, kidneys, and heart was assessed (**Fig. 14**). Notably, the bacterial burden in the spleen of the mice that received no antibiotic was found to be reduced by approximately 3-log compared to pretreatment levels, an effect ascribed to activity of the immune system of the mice in this study. While vancomycin (25 mg/kg, IV, q12h) significantly reduced the spleen burden relative to the vehicle treated group, compound **7** administered at the same dose (25 mg/kg, IV, q12h) further reduced bacterial burden by approximately 1-log fold (**Fig. 14A**, see **Table S9** and **S10** for individual data and statistical analysis). In the kidneys, the bacterial burden in the vehicle treated group increased relative to pretreatment levels and a clear antibiotic affect was observed for both vancomycin and compound **7**. In the vancomycin treatment group (25 mg/kg, IV, q12h) a near 4-log decrease in bacterial burden was measured relative to the vehicle treated group. By comparison, the same dosing of compound **7** was found to more effectively reduce the kidney burden, resulting in an almost 6-log decrease compared to vehicle. Furthermore, a lower total dose of compound **7** (10 mg/kg, SC, q6h) also outperformed vancomycin, reducing the kidney burden >1-log fold more (**Fig. 14B**, see **Table S11** and **S12** for individual data and statistical analysis). In the heart, vancomycin (25 mg/kg, IV, q12h) and compound **7** (dosed at either 25 mg/kg, IV, q12h, or 10 mg/kg, SC, q6h) caused similar significant reductions in bacterial burden (~3-log fold compared to vehicle) (**Fig. 14C**, see **Table S13** and **S14** for individual data and statistical analysis). The effectiveness of compound **7** in clearing *S. aureus* infection in the heart points to the potential for the guanidino lipoglycopeptides to be used in the treatment of infective endocarditis (IE), a condition commonly related to *S. aureus* biofilm formation[14] which compound **7** is also able to successfully inhibit/eradicate *in vitro*. Clinically, the treatment of IE presents a major challenge with a 20% morbidity rate in the first 30 days of disease.[37] While glycopeptide therapy with dalbavancin has recently been reported as a promising treatment option for IE,[38,39] non-susceptible strains and glycopeptide induced IE have also been reported,[40,41] underscoring the need for new and effective treatments.

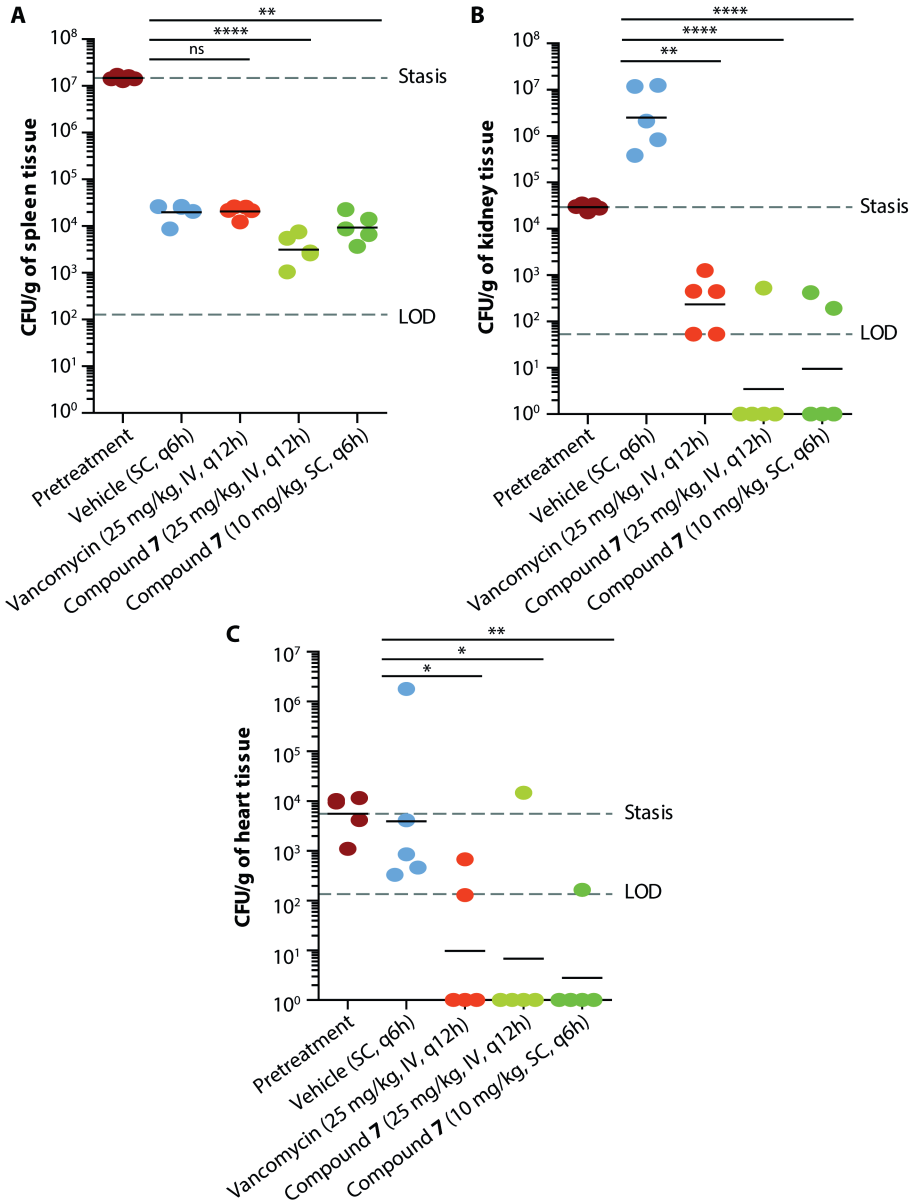

Fig. 14. *In vivo* efficacy of guanidino lipoglycopeptide 7 in murine sepsis burden studies. (**A**) Spleen, (**B**) kidney, and (**C**) heart burden following infection with *S. aureus* NCTC8178 in healthy mice. Starting 1 h post-infection immunocompetent mice were treated for 24 h. Mice were monitored for a total of 49 h after which they were euthanized and the spleen, kidneys, and heart were removed and weighed. Tissue samples were homogenized and cultured on MSA agar at 37 °C for 18-24 h followed by colony counting. Each group consisted of n=5 mice. LOD = Limit of detection. q indicates dosing interval. ns = non-significant, *p=0.1-0.01, **p=0.01-0.001, ***p=0.001-0.0001, and ****p≤0.0001. Bar = geometric mean.

3.3 Conclusions

To tackle the high AMR-related morbidity and mortality related to Gram-positive organisms,[1,42,43] we reported the synthesis and potent *in vitro* antibacterial activity of a novel semi-synthetic glycopeptide antibiotic class, the guanidino lipoglycopeptides (**Chapter 2**). Also of note is the finding that addition of serum to the media used in the MIC assays has little impact on the activity of most guanidino lipoglycopeptides (**Table 1**). This is indicative of low plasma protein binding and suggestive of high compound availability *in vivo*.[10,11,44–48] In addition to inhibiting exponentially growing bacteria, compound **7** also proved to be a potent *S. aureus* biofilm inhibitor and eradicator (**Table 3**). While the guanidino lipoglycopeptides display enhanced antibacterial activity, this is not due to accelerated killing kinetics as indicated by the similarity in the time-kill curves obtained with the clinically used glycopeptides vancomycin,[49,50] teicoplanin,[49] telavancin,[50] and dalbavancin[50] (**Fig 2**). The guanidino lipoglycopeptides also demonstrate a low propensity for resistance selection. This is in contrast to the clinically used lipopeptide daptomycin, which selects for resistance in the same strains of VRE and MRSA used in a 30-day serial passage assay (**Fig. 3**). Furthermore, in cell-based studies, the guanidino lipoglycopeptides, and particularly compound **7**, demonstrate a favorable toxicity profile relative to the clinically used lipoglycopeptides telavancin and oritavancin. Specifically, compound **7** is non-hemolytic (**Fig. 1**) and shows little effect on human kidney and liver cells while telavancin and oritavancin both exhibit appreciable levels of toxicity (**Table 2**). Collectively, the enhanced antibacterial activity observed for the guanidino lipoglycopeptides along with their favorable toxicity profile, suggests that this novel class of antibiotics might have a larger therapeutic window relative to current clinically used glycopeptides.

Mechanistically, the guanidino lipoglycopeptides maintain the lipid II dependent mechanism of action common to all glycopeptides causing inhibition of late-stage cell wall biosynthesis. Of particular note is the finding that the binding affinity of compound **7** for LII-D-Ala is nearly 10-times greater than that of vancomycin, providing an explanation for the increased antibacterial activity observed (**Fig. 6**). Compound **7** also maintains strong binding to the mutant form of lipid II (LII-D-Lac) most commonly associated with vancomycin resistance. In fact, compound **7** binds LII-D-Lac more tightly than vancomycin binds native LII-D-Ala (**Fig. 6**, **Table S2**). These findings can explain the observation that the guanidino lipoglycopeptides retain their potent activity against vancomycin-resistant strains. While the specific molecular level details of how the guanidino lipoglycopeptides achieve a stronger binding interaction with lipid II remain to be fully elucidated, we speculate that the substituted guanidino motif provides a beneficial combination of productive electrostatic interactions with the negatively charged bacterial cell surface and hydrophobically-driven membrane anchoring. In addition to their

established lipid II binding, lipoglycopeptides have been reported to have membrane-targeting effects.[4,20,27–29] Among the guanidino lipoglycopeptides evaluated, we found that compound **7** is notable in that it does not display significant levels of non-specific membrane activity as evidenced by its low propensity to cause membrane permeabilization or depolarization (**Fig. 9, Fig. 10**). The absence of such effects is typically seen as favorable trait, given that antibacterial agents that function via membrane disruption are often linked to perturbation of mammalian cell membranes leading to off-target effects and toxicity.[29,35]

Based on the outcomes of the various *in vitro* investigations performed with the guanidino lipoglycopeptides, compound **7** was selected for further *in vivo* evaluation. Compound **7** exhibits potent and dose-dependent efficacy in an MRSA murine thigh infection model and two *S. aureus* sepsis studies (**Fig. 12**, **Fig. 13**, and **Fig. 14**). The *in vivo* activity of compound **7** is consistently superior to that of vancomycin in both reducing bacterial thigh burden as well as increasing 7-day survival. Investigation of the organ-specific effects of compound **7** also shows it to be superior to vancomycin in reducing the infection burden in the spleen, kidney, and heart.

In summary, we here report the development of the guanidino lipoglycopeptides, a promising new class of semisynthetic glycopeptide antibiotics. To date, telavancin is the only approved semisynthetic vancomycin analogue used in the clinic and carries with it serious toxicity concerns. The *in vitro* and *in vivo* studies performed with the guanidino lipoglycopeptides, specifically compound **7**, demonstrate the potent antibacterial activity and promising toxicity profiles of this new class of semisynthetic glycopeptides. Further assessment of the guanidino lipoglycopeptides using advanced *in vivo* models will be the next step towards a more complete characterization of their toxicity and PK profiles *en route* to establishing their clinical potential in the treatment of serious Gram-positive infections.

3.4 Experimental Methods

Serum reversal assay. Serum reversal assays were performed according to the broth microdilution protocols described in **Chapter 2** using 50/50 TSB/sheep serum + 0.002% p80 as growth medium once bacteria were added to the antibiotic serial dilution and onward.

Hemolysis assay. Whole defibrinated sheep blood was centrifuged for 15 min at 4 °C (400 g). The top layer was discarded and the bottom layer was washed with phosphate buffered saline (PBS) and centrifuged for 15 min at 4 °C (400 g). Washing cycles were repeated at least three times. In polypropylene 96-well microtiter plates, serial dilutions of

antibiotics in PBS with 0.002% p80 in triplicates were added (75 µL) and an equal volume of packed blood cells diluted 25-fold in PBS with 0.002% p80 (75 µL) was added to all wells. Plates were incubated for 18 h at 37 °C with continuous shaking (500 rpm). After incubation, plates were centrifuged for 5 min (800 g) and 25 µL of supernatant was transferred to a clear UV-star flat-bottom polystyrene 96-well plate already containing 100 µL H_2O per well. Absorption was measured at 415 nm. Data were corrected by subtraction of the background response of 1% DMSO in the presence of cells with no antibiotic and normalized using the absorbance of 0.1% Triton X-100 with blood cells as 100% hemolysis control. In two separate experiments, the optimal wavelength for the hemolysis assay was determined by doing a full scan and the linear detection range was determined to ensure correct interpretation of the data.

Mammalian cytotoxicity assay. Compound cytotoxicity was evaluated against HepG2 and HEK293T human cell lines using a standard (3-(4,5-dimethylthiazol-2-yl)−2,5-diphenyltetrazolium bromide (MTT) assay protocol. Briefly, HepG2 and HEK293 cells were seeded at a density of 1.5×10^4 cells per well in a clear 96-well tissue culture treated plate in a final volume of 100 µL in Dulbecco's Modified Eagle Medium (DMEM), supplemented with FBS (1%), Glutamax and Pen/Strep. Cells were incubated for 24 h at 37 °C, 7% CO_2 to allow cells to attach to the plates. In addition to a single vehicle control, compounds (diluted from DMSO stock) were added into each well at eight concentrations ranging from 100 µM to 0.046 µM in three-fold dilutions (final DMSO concentration 0.5%) following incubation for 24 h at 37 °C, 7% CO_2. After the incubation, MTT was added to each well at a final concentration of 0.40 mg/mL. The plates were then incubated for 2 h at 37 °C, 7% CO_2. Medium was carefully removed via suction, and the purple formazan crystals were resuspended in 100 µL DMSO. Absorbance was read at 570 nm using a Clariostar plate reader. Data analysis was done with GraphPad Prism software. CC_{50} values were calculated using non-linear fitted curve with variable slope settings, with values adjusted for background (plotted $ABS_{SAMPLE} = (ABS_{SAMPLE} - ABS_{BACKGROUND}) / (ABS_{VEHICLE} - ABS_{BACKGROUND})$). The experiment was performed with biological duplicates and technical triplicates.

Time-kill assay. From glycerol stocks, bacterial strains were cultured on blood agar plates and incubated overnight at 37 °C. Subsequently, a single colony was cultured in TSB + 0.002% p80 overnight at 37 ºC. The culture was diluted 100-fold in fresh media and grown until early exponential phase (OD_{600}=0.2-0.4) followed by dilution in media to OD_{600}=0.0025. The culture was split in separate culture tubes containing 2 mL. Antibiotics were added to the cultures (at the concentrations indicated in the experiments results) and incubated at 37 ºC for a total of 24 h. At indicated time points (t=0, t=1, t=2, t=4, t=8, and t=24h), 100 µL of each culture was transferred to eppendorf tubes and centrifuged for 5 min (10,000 rpm). The supernatant was removed and the cell pellets

were resuspended in an equal volume of 0.9% NaCl in H_2O (filter-sterilized). The samples were serial diluted with a 10-fold factor in filter-sterilized 0.9% NaCl in H_2O. Of these serial dilutions the 100-fold, 1,000-fold, 10,000-fold, and 100,000-fold dilution were plated out on blood agar plates (20 µL) in technical duplicates, subsequently allowed to evaporate and incubated at 37 ºC for 24 h. The colonies were counted and used to calculate the CFU/mL remaining in the original culture by taking the dilution factors into account. Experiment was performed in biological duplicates.

Resistance selection assay. From glycerol stocks, bacterial strains were cultured on blood agar plates and incubated overnight at 37 °C. A single colony was grown to exponential phase (OD_{600}=0.5) in TSB + 0.002% p80 and diluted 100-fold in fresh media. In polypropylene 96-well microtiter plates, antibiotics were added in biological triplicates and serial diluted 2-fold by transfer and mixing from one well to the next to achieve a final volume of 50 µL per well. An equal volume of bacterial suspension was added to the wells and plates were sealed with a breathable seal and incubated overnight at 37 ºC. The next day, bacterial cultures corresponding to 0.25xMIC were diluted 100-fold in fresh media and added (50 µL per well) to a newly prepared antibiotic dilution series (50 µL per well) followed by overnight incubation at 37 ºC. This procedure was repeated for 30 days and the MIC was recorded daily. Cultures containing daptomycin were supplemented with 50 mg/L $CaCl_2$ and 10 mg/L $MgSO_4$. The experiment was performed in biological replicates and for each replicate the MIC was determined from the median of a minimum of triplicates.

Determination of MBEC and MBIC. The ability of the compounds to destroy established, preformed bacterial biofilms was determined using MBEC Assay Biofilm Inoculators with 96-well base.[51] The MBEC was defined as the lowest concentration able to sterilize a biofilm, that was established for 24h, after 24h of antibiotic treatment. For MBEC determination, the manufacturers protocol was adjusted for use with *S. aureus* ATCC25923.[32,51] In brief, MBEC plates were inoculated with 150 µL of culture adjusted to 10^6 CFU/mL in TSB supplemented with 0.5% glucose and incubated for 24h at 110 rpm, 37 °C and 60-80% humidity to allow biofilm formation. The CFU/mL from the inoculum was checked to ensure the correct starting cell count. Following incubation MBEC peg lids were washed in sterile saline for 10 sec and transferred to a fresh 96-well plate containing 200 µL per well of antibiotic dilutions in TSB supplemented with 0.5% glucose and 0.002% p80. Plates were treated for 24h before the peg lid was transferred to a fresh recovery plate containing 200 µL of TSB and sonicated for 30 min to remove residual biofilm from the pegs. MICs and MBCs were determined from planktonic cells and the recovery plate was incubated for 24h. The first well from the antibiotic dilution not showing visible cell growth was determined to be the MBEC. OD was measured in the Tecan Spark M plate reader at 650 nm to confirm the visible results.

To determine if the compounds are able to inhibit biofilm formation in the MBEC peg lid system, the protocol was adjusted in the way that antibiotic dilutions were added directly with the cells before biofilm formation, allowing determination of the MBIC. To confirm biofilm formation, biofilm cell numbers were determined by removing control pegs from the peg lid after incubation and recovering cells in TSB by sonication and spot plating.

UDP-MurNAc-pp accumulation assay. From glycerol stocks, *S. aureus* ATCC29213 was cultured on blood agar plates and incubated overnight at 37 °C. A single colony was grown in TSB + 0.002% p80 overnight at 37 °C and diluted 100-fold in fresh media. The bacterial culture was grown at 37 °C until exponential phase (OD_{600} = 0.5). Chloramphenicol was added at a final concentration of 130 µg/mL and the culture was incubated for an additional 15 min at 37 °C. Next, the culture was split in 5 mL cultures and test antibiotics were added at a final concentration of 5 µM. The cultures were incubated at 37 °C for 1 h after which they were centrifuged for 5 min at 4 °C to pellet the bacteria (3,900 rpm). The supernatant was removed and the pellets were resuspended in 1 mL H_2O. The samples were boiled at 100 °C for 15 min and subsequently centrifuged for 30 min (12,000 rpm). The supernatant of the samples was lyophilized and redissolved in 250 µL buffer A (50 mM ammonium bicarbonate, 5 mM NEt_3, pH 8.3). Samples were analyzed by analytical RP-HPLC at 254 nm using a 0-25% buffer B (MeOH) gradient over 25 min. The HPLC analysis was done using a Phenomenex Jupiter su C_{18} 300 Å column (250x4.60 mm, 5 µm) on a Shimadzu LC-2030 Plus instrument.

Assessment of cell wall integrity and deformation of B. subtilis. Cell wall integrity and deformation of *B. subtilis* 168 cells were analyzed as previously described.[52] Cultures were grown in MHB at 30 °C and treated with 5xMIC of vancomycin, **7**, or oritavancin for 30 min after reaching OD_{600}=0.3. Following incubation, cells were fixed in 1 mL of acetic acid and methanol (1:3 (v:v)). 0.5 µL of fixed cells were transferred onto agarose slides with 1% (w/v) agarose and pictured with a Zeiss Axio Observer Z1 microscope (Zeiss, Jena, Germany) combined with HXP 120 V light source and an Axio Cam MR3 camera. Images were taken with ZEN 2 software (Zeiss). Analysis of pictures was performed with ImageJ v1.45s software (National Institutes of Health).

Purification of cell wall precursor LII- D-Ala and LII-D-Lac. Lipid II ending in D-Ala-D-Ala and D-Ala-D-Lac was synthesized and purified according to published protocols.[24,53,54] Briefly, lipid II synthesis reactions were performed with 2 µmol $C_{55}P$ in a buffer composed of Tris/HCl pH 7.5, Triton X100, $MgCl_2$, UPD-GlcNAc, *M. luteus* membrane preparations, and either UDP-MurNAc-pentapeptide from *S. simulans* (for lipid II ending in D-Ala) or UDP-MurNAc-depsipeptide from *Lactobacillus casei*

ATCC393 (for LII-D-Lac). The product was purified via HPLC, lyophilized, resuspended in chloroform/methanol (1:1), and stored at -20 °C. For purification of UDP-MurNAc-depsipeptide, MRS broth was inoculated to 1% with a *L. casei* preculture and incubated at 37 °C to OD_{600}=0.6. Chloramphenicol was added in a concentration of 65 µg/mL to inhibit protein translation and cell lysis, and cultures were incubated for 15 min at 37 °C. 0.5 mM $ZnCl_2$ and 40 µg/mL bacitracin were used to induce UDP-MurNAc-pentapeptide accumulation. Following incubation for 60 min at 37 °C cells were harvested, extracted with boiling H_2O, and centrifuged. The supernatant was lyophilized and redissolved in H_2O.

Lipid II antagonization assay. Lipid II in chloroform was added to a polypropylene 96-well plate (5-fold molar excess compared to test antibiotics) and the chloroform was allowed to evaporate. Test antibiotics (50 µL, 16xMIC) were mixed with the 5-fold molar excess of pure LII-D-Ala in triplicates in the plate as well as added to the plate in triplicates without LII-D-Ala present. *S. aureus* ATCC29213 colonies from fresh blood agar plates were suspended in TSB + 0.002% p80 by direct colony suspension to an OD_{600} of 0.5. The bacterial suspension was diluted 100-fold in TSB + 0.002% p80 and 50 µL was added to the test compounds in the microtiter plate to achieve a final concentration of 8xMIC for all test compounds. The samples were incubated at 37 ºC for 24 h with constant shaking (600 rpm) and subsequently inspected for visible bacterial growth.

Formulation of large unilamellar vesicles (LUVs). Phospholipid stock solutions (10-30 mM) were prepared in chloroform. Gram-positive LII-D-Ala and LII-D-Lac stock solutions (1 mM) were prepared in chloroform/methanol 1:1. Appropriate volumes of the stock solutions were mixed, and the organic solvents evaporated under a stream of nitrogen at 35-40 ºC. The resulting dry lipid films were hydrated with buffer (20 mM HEPES, pH 7.4) and homogenized by 5 cycles of freezing (-196 ºC) and thawing (35-40 ºC) to produce vesicle suspensions with a final concentration of 10 mM total lipid. The suspensions were passed through 2 opposite directed Whatman® polycarbonate membranes with a final pore size of 0.2 µm (Sigma Aldrich, Taufkirchen, Germany) 11 times at room temperature with an Avanti mini extruder (Avanti Polar Lipids Inc., Alabaster, Alabama USA) to yield homogeneous LUV suspensions.

Isothermal Titration Calorimetry (ITC). Large unilamellar vesicles (LUV) suspensions of DOPC or 1:3 DOPG/DOPC with or without 100 or 200 µM LII-D-Ala or LII-D-Lac (10 mM total lipid) were titrated into a freshly prepared glycopeptide solution in the same buffer. Control titrations included the titration of buffer into glycopeptide and LUVs into buffer. All binding experiments were performed using a MicroCal PEAQ-ITC Automated microcalorimeter (Malvern Panalytical Ltd, Malvern, UK). The samples were equilibrated to 25 ºC prior to measurement. The titrations were conducted at 25 ºC under

constant stirring at 1,000 rpm. Each experiment consisted of an initial injection of 0.3 µL followed by 25 separate injections of 1.5 µL into the sample cell of 200 µL. The time between each injection was 180 seconds and the measurements were performed with the reference power set at 5 µcal/s and the feedback mode set on "high". The calorimetric data obtained were analyzed using MicroCal PEAQ-ITC Analysis Software Version 1.20 (Malvern Panalytical Ltd, Malvern, UK). ITC data fitting was made based on the "One set of sites" fitting model of the software. The best fit is defined by chi-squared minimization. Thermodynamic parameters are reported as the mean ± SD of three experiments.

Construction of S. aureus vraRS reporter strain. The promoter region of the VraRS two-component system was cloned into the pXEN1 vector, which contains the luciferase *luxABCDE* operon, using the *EcoRI* and *BamHI* restriction sites. Those sites were inserted in the *vraRS* promoter sequence using the forward primer 5'-GCGCGGAATTCACGGTGCTATTTGTGCGCC-3' (PvraSR_EcoRI-FW) and the reverse primer 5'- GCGCGGGATCCCACGTTCAACATAGTTCATAACTA-3' (PvraSR_BamHI-RV). *S. aureus* RN4220 was transformed with the final vector via electroporation and the clones were selected on MH agar plates containing 5 µg/mL chloramphenicol.

B. subtilis and S. aureus cell wall stress response and antagonization with purified lipids. The cell wall stress response was assessed using *B. subtilis 168* strain TMB1617 and *S. aureus* RN4220 that express the *Photorhabdus luminescens* luciferase under the promoter P_{liaI}-lux[23] and P_{vraRS}-lux respectively. Cultures were grown in MHB with 5 µg/mL chloramphenicol and subjected to a serial dilution of antibiotic supplemented with 0.002% p80. Vancomycin and oritavancin were used as controls. Antagonization of cell wall stress response with LII-D-Ala and LII-D-Lac was analyzed using a protocol described previously[24] with slight modifications. Purified lipids were subjected to antibiotic in different molar lipid/compound ratios (2:1, 4:1, 8:1) and incubated at RT for 15 min before addition of *B. subtilis* luciferase reporter culture at OD_{600}=0.5. Luminescence was measured every 15 min for 10 h using the Tecan Spark 10 M microplate reader.

Complex formation with cell wall precursors. Purified LII-D-Ala and LII-D-Lac were analyzed for complex formation with glycopeptide antibiotics at increasing concentrations. 2 nmol of lipid II variant was incubated with 2-16 nmol of guanidino lipoglycopeptide or 4 nmol of control antibiotics vancomycin or oritavancin in 50 mM Tris/HCl, pH 7.5 supplemented with 0.002% p80. Incubation was conducted at RT for 30 min and unbound lipids were extracted using n-butanol/pyridine acetate (2/1, vol/vol) at pH 4.2.[54,55] The butanol phase was spotted onto a TLC plate and developed in solvent

composed of $CHCl_3$/MeOH/H_2O/NH_3 (88:48:10:1, v/v/v/v).[56] Lipids were visualized using phosphomolybdic acid staining.

In vitro inhibition of cell wall biosynthesis reactions with LII-D-Ala and LII-D-Lac. The influence of glycopeptides on the PBP2 catalyzed transglycosylation of lipid II was analyzed using purified PBP2 as described previously with modifications.[57] In short, 2 nmol of LII-D-Ala/LII-D-Lac was resuspended in 100 mM MES, pH 5.5, 10 mM $MgCl_2$ and 2 mM Ca^{2+} supplemented with 0.002% p80. **7** was added at molar ratios of 1:1, 2:1, and 10:1 with respect to the lipid II. Oritavancin was used as a control. Antibiotics and lipids were incubated for 15 min before addition of purified PBP2. A negative control, lacking treatment and enzyme, and a positive control, containing PBP2 but lacking the compound, were added for comparison. Enzymatic reactions were conducted at 30 °C for 2 h. Free lipids were extracted and visualized as described for the complexation assays. Inhibition of the enzymatic complex MurTGatD was assessed in 160 mM Tris-HCl, 50 mM KCl, 40 mM $MgCl_2$, 0.26% Triton X-100, 6.6 mM glutamine, 1.25 mM $CaCl_2$, 6 mM ATP, and 0.002% p80. 2 nmol of the lipid II variant was used in a final volume of 30 µL.[58] Purified MurTGatD complex was added to start the reaction. Compounds were added in the same molar ratios as described for PBP2 inhibition and incubation, extraction, and staining were performed according to the above described procedure as well. Lipid II was quantified for pixel density using ImageJ.

Membrane depolarization assay. From glycerol stocks, MRSA USA300 was cultured on blood agar plates and incubated overnight at 37 °C. A single colony was grown in LB media overnight and was diluted 100-fold in fresh media. The cells were grown at 37 °C to early exponential phase. Cells were pelleted (10,000 rpm, 5 min) and washed with filter-sterilized 10 mM HEPES buffer (pH 7.4) supplemented with 50 µg/mL $CaCl_2$ and 5 mM glucose. Supernatant was removed and cell pellets were resuspended in the same buffer at a desired cell density. 100 µL of 6 µM $diSC_3(5)$ dye was added to a clear flat-bottom polystyrene 96-well plate and fluorescence was monitored for 15 min at 37 °C collecting data every 1 minute at excitation/emission 643/666 nm using a Biotek SynergyMx. Next, 98 µL of cells were added to the wells (final OD_{600}=0.15-0.3) and data collection continued for 3 min at 37 °C. Last, antibiotics were added to achieve a final concentration of 1.5 µg/mL, 8 µg/mL, or 16 µg/mL (2 µL) and fluorescence was monitored on the Biotek SynergyMx (excitation/emission 643/666 nm) at 37 °C for 30 minutes collecting data every 1 min. The final concentration of $diSC_3(5)$ dye in all wells was 3 µM. Note that no p80 was supplemented to the media or buffer in this assay, likely altering the MIC of the compounds. Data were corrected by subtraction of the background response of $diSC_3(5)$ in the presence of cells with no antibiotic. Each sample was tested in triplicates.

Membrane permeabilization assay. From glycerol stocks, MRSA USA300 was cultured on blood agar plates and incubated overnight at 37 °C. A single colony was grown in LB media overnight and was diluted 100-fold in fresh media. The cells were grown at 37 °C to early exponential phase. Cells were centrifuged (10,000 rpm, 5 min) and washed with 10 mM HEPES buffer (pH 7.4) supplemented with 50 µg/mL $CaCl_2$ and 5 mM glucose. Supernatant was removed and cells were resuspended in the same buffer at an appropriate cell density. Propidium iodide (PI) dye (final concentration of 10 µM), cells (final OD_{600}=0.15-0.3) and antibiotics (final concentration of 1.5 µg/mL, 8 µg/mL, or 16 µg/mL) were added to a total volume of 100 µL into a black flat-bottom 96-well plate. Fluorescence was monitored at excitation/emission 535/620 nm at 37 °C on a Biotex SynergyMx for 30 min collecting data every 1 min. Note that no p80 was supplemented to the media or buffer in this assay, likely altering the MIC of the compounds. Data were corrected by subtraction of the background response of PI dye in the presence of cells with no antibiotic. Each sample was tested in triplicate and data ware analyzed with Prism software.

Delocalization of GFP-MinD. The impact of compound **7** on membrane potential was analyzed as described previously using fluorescence microscopy and *B. subtilis* 1981 erm spc minD::ermC amyE::Pxyl-gfp-minD that is characterized by gfp-minD under the P_{xyl} promotor.[34,59] The strain was grown at 30 °C in LB supplemented with 0.1% w/v xylose and 50 µg/mL spectinomycin. At OD_{600}=0.25 cells were treated with 5xMIC of compound. Nisin was used as a positive control. Samples were taken at different time-points (2, 5, 15, 30, and 60 min), transferred onto microscope slides with 1% (w/v) agarose and pictured with a Zeiss Axio Observer Z1 microscope (Zeiss, Jena, Germany) combined with HXP 120 V light source and an Axio Cam MR3 camera. Images were taken with ZEN 2 software (Zeiss). Analysis of pictures was performed with ImageJ v1.45s software (National Institutes of Health).

In vivo studies – Animal ethics, strain and housing. Animal experiments were performed in an AAALAC-accredited animal facility under the authority of UK Home Office Establishment, Project and Personal Licences, with local ethical committee clearance. All studies were prepared and conducted in keeping with the ARRIVE Guidelines. Male CD1 specific pathogen free mice (Charles River, Margate UK) were used (total of n=116 mice for all studies), weighed 26.6-35.5 gram (for the tolerability, PK, and thigh model) or 25.0-32.6 gram (for the sepsis burden and survival model) at study start. Mice were allowed to acclimatize for at least 7 days. Mice were housed in sterilized individually ventilated cages in groups of 3-5 mice supplied with HEPA filtered air and aspen chip bedding (changed a minimum of once a week). Food (SDS, Whitham, UK) and water were available *ad libitum*. The room temperature was 22 °C ± 1 °C, with a 60% relative humidity and a maximum background noise of 56 dB. Mice were exposed to a 12 h

light/dark cycle. Cages of mice were assigned to study groups randomly. No animals or values were excluded from analyses.

In vivo studies – Preparation of compound for in vivo studies. Vehicle for all studies was 10% DMSO in sterile water for injection (WFI) and was clear and colorless. Compound **7** was prepared by adding DMSO to 10% of the desired volume of diluent, ensuring the test article was in solution and then slowly adding WFI to the final volume. The mixture was solubilized by vortexing and formed a clear colorless solution. In case of vancomycin two preparation protocols were in place: 1) for tolerability, PK and thigh infection it was prepared by adding 10 mL of WFI to 500 mg vancomycin to produce a clear colorless stock solution at 50 mg/mL. The stock solution was then diluted 1:10 in WFI to 5 mg/mL and administered at 5 mL/kg. 2) For the sepsis studies, vancomycin solution was prepared by adding saline for injection (SFI) to vancomycin to produce a clear and colorless stock solution at 5 mg/mL.

In vivo studies – In vivo tolerability. Tolerability of compound **7** was assessed at 10 mg/kg (n=2), 30 mg/kg (n=2) and 50 mg/kg (n=1) and 100 mg/kg (n=1) by intravenous (IV) injection at 5 mL/kg and at 100 mg/kg (n=2) by subcutaneous (SC) injection at 5 mL/kg (in 10% DMSO in WFI) in naïve mice (n=8 total).

In vivo studies – In vivo pharmacokinetics. Compound **7** was administered at 3 mg/kg SC at 5 mL/kg in naïve mice (n=3). Whole blood (20 µL per sample) was collected from the lateral tail vein by tail prick sampling at 5 min, 15 min, 30 min, 1 h, 2 h, and 4 h into EDTA coated glass capillary tubes. An 8 h sample was taken via terminal cardiac puncture under isoflurane anesthesia into an EDTA blood tube. Each 20 µL blood sample was mixed with 20 µL sterile water prior to freezing at -80 °C. PK analysis was performed by a generic LC-MS/MS method and samples were quantified using matrix matched calibrators. Samples were prepared for bio-analysis via protein precipitation. Blood concentration vs time data and relevant PK parameters were reported following non-compartmental analysis (NCA).

In vivo studies – In vivo MRSA thigh infection model. In vivo efficacy was determined in a murine thigh infection model. A total of n=30 mice was used in this study, with each group consisting of n=6 mice with both thighs infected (n=12 thighs per treatment group) and each thigh was treated as a separate sample even though they are not completely independent samples.

Immunosuppression. Mice were rendered neutropenic by a SC injection of 150 mg/kg and 100 mg/kg cyclophosphamide 4 days and 1 day before infection respectively.

The immunosuppression regime leads to neutropenia starting 24 h post administration of the first injection, which continues throughout the study.

Infection. An aliquot of a previously prepared frozen stock of the bacterial strain *S. aureus* NRS384 in log phase was thawed and diluted in sterile PBS to the desired inoculum just prior to infection. Mice were infected in both thighs with 0.05 mL of the MRSA USA300 strain *S. aureus* NRS384 (1.47×10^6 CFU/mL, 7.33×10^4 CFU per thigh) intramuscularly under temporary inhaled anesthesia (2.5% isoflurane in oxygen for 3-4 minutes). Analgesia was provided at infection and every 8-12 h via buprenorphine administration through SC injection at 0.03mg/kg.

Treatment. Mice were administered vehicle control every 6 h SC at 5mL/kg, 25 mg/kg positive control vancomycin every 12 h IV at 5 mL/kg, or 3 mg/kg or 10 mg/kg compound **7** every 6 h SC at 5mL/kg, starting 1 h post-infection.

Endpoints. Pretreatment group (n=6) endpoint was 1 h post-infection. The other treatment groups had a 25 h planned endpoint, which became 23 h due to mice (in vehicle group) reaching clinical endpoint. The clinical condition of all animals was assessed prior to humane euthanasia using pentobarbitone overdose, and the thighs removed and weighed. Weighed thighs were homogenized in 3 mL sterile PBS containing 10% glycerol in Precellys bead beater tubes in a Precellys Evolution homogenizer and quantitatively cultured on MSA agar using the Miles and Misra method at 37 °C for 18-24 h followed by colony counting.

Data analysis. Data analysis was performed with StatsDirect software v. 3.2.8 using non-parametric statistical models (Kruskal-Wallis using Conover-Inman to make all pairwise comparisons between groups). For all calculations, the thighs from each animal were treated as two separate data points even though they are not completely independent samples.

In vivo studies – In vivo sepsis models. In vivo efficacy was determined in a mouse model of *S. aureus* NCTC8178 disseminated sepsis. The study was split into two: a survival model and a burden model. A total of n=50 mice was used in the survival study, with each group consisting of n=10 mice. A total of n=25 mice was used in the burden study, with each treatment group consisting of n=5 mice and from each mouse the spleen, kidney, and heart were harvested.

Infection. The bacterial strain *S. aureus* NCTC8178 (Newman strain) was prepared from an overnight Mueller Hinton broth which was sub-cultured and shaken at 37 °C at 300 rpm until it reached log phase. Mice were infected with 0.1 mL of the

bacterial strain suspensions by IV injection. The inoculum was 3.3 x 10^7 CFU/mouse for the 7-day survival model and 1.8 x 10^7 CFU/mouse for the 48 h burden study.

Treatment. For the survival model – starting 1 h post-infection mice were administered for the first 24 h with either vehicle control every 6 h SC at 5mL/kg, or 25 mg/kg vancomycin positive control or compound **7** every 12 h IV at 5mL/kg, or 3 mg/kg or 10 mg/kg compound **7** every 6 h SC at 5mL/kg. For the burden model – starting 1 h post-infection mice were administered for a total of 24 h with vehicle control every 6h SC at 5mL/kg, 25 mg/kg positive control vancomycin or compound **7** every 12 h IV at 5mL/kg, or 10 mg/kg compound **7** every 6 h SC at 5mL/kg.

Endpoints. For the survival model the endpoint was seven days (169 h) or when animals reached clinical endpoint, whichever was sooner. The clinical condition of animals was assessed prior to humane euthanasia using pentobarbitone overdose. No organ culture was performed for the survival study. For the burden model the endpoint was 1 h (for pretreatment group, n=5) and 49 h (other groups) post-infection, the clinical condition of all animals was assessed prior to humane euthanasia using pentobarbitone overdose, and the spleen, kidneys and heart removed and weighed. Tissue samples were homogenized in 2 mL ice cold sterile PBS; the homogenates were quantitatively cultured onto MSA agar using the Miles and Misra method and incubated at 37 °C for 18-24 h before colonies were counted.

Data analysis. Survival data were analyzed by Logrank survival analysis using StatsDirect statistical software v 3.3.4 and compared to vehicle control. The data from the culture burdens were analyzed using appropriate non-parametric statistical models (Kruskal-Wallis using Conover-Inman to make all pairwise comparisons between groups) with StatsDirect software v. 3.3.4, and compared to vehicle control. Samples with burden below limit of detection were given a value of 1 for graphical and statistical purposes.

3.5 Supplementary Information

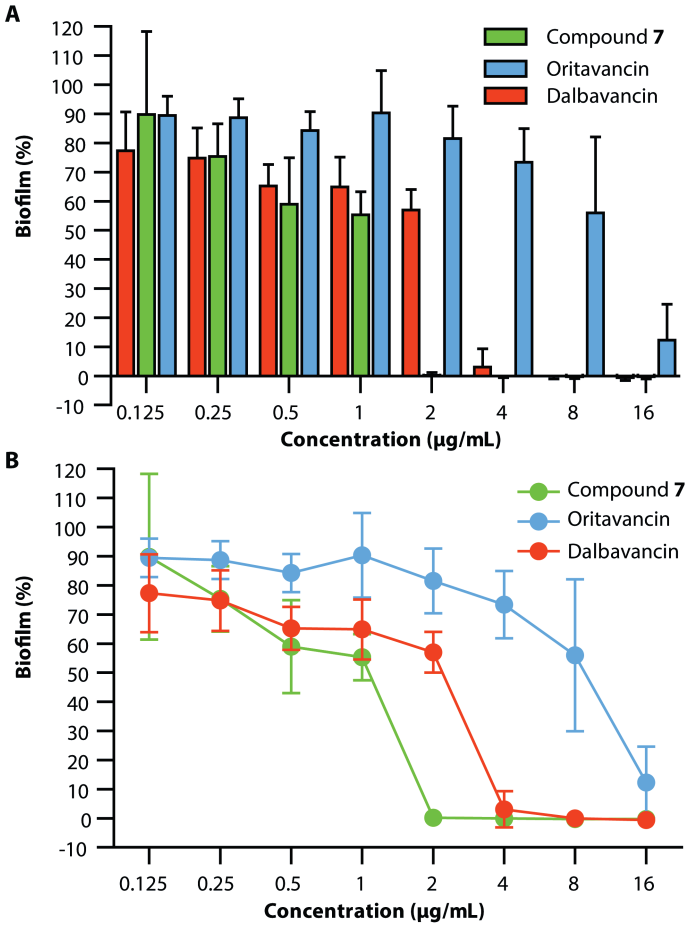

Fig. S1. Effect of glycopeptides on eradication of preformed biofilm. (**A**) Bar and (**B**) line graph of MBEC determined by treatment of a preformed biofilm with compounds in serially diluted concentrations. *Experiment performed by Melina Arts/Stefania De Benedetti.*

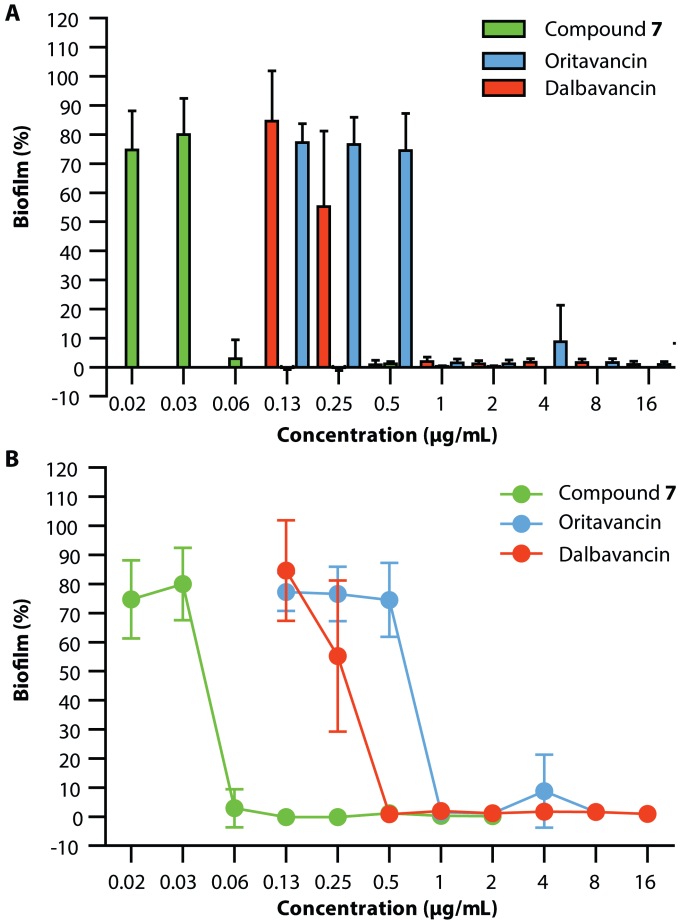

Fig. S2. Effect of glycopeptides on biofilm formation. (**A**) Bar and (**B**) line graph of MBICs determined by addition of compounds with the inoculum. Values represent biological duplicates with technical quadruplicates. Data represent mean ± SD. *Experiment performed by Melina Arts/Stefania De Benedetti.*

Table S1. Antagonization of guanidino lipoglycopeptides by LII-D-Ala.

Compound	Visible bacterial growth at 8xMIC	
	Without free lipid II present	With free lipid II present (5-fold molar excess)
Vancomycin (**1**)	-	+
Telavancin (**3**)	-	+
Compound **7**	-	+
Compound **8**	-	+
Compound **9**	-	+
Compound **16**	-	+
Compound **18**	-	+

Antagonization of the activity of vancomycin, telavancin, and selected guanidino lipoglycopeptides at 8xMIC by a 5-fold molar excess of lipid II with D-Ala-D-Ala terminus. '-' Indicates no visible bacterial growth, '+' indicates visible bacterial growth. Experiment performed in a minimum of triplicates.

Table S2. Thermodynamic parameters of glycopeptides binding to LII containing LUVs by ITC.

	Compound **7**		Vancomycin (**1**)	
LII (type)	D-Ala	D-Lac	D-Ala	D-Lac
LII (μM)	100	200	200	200
1 or **7 (μM)**	20	40	10	10/20
K_D (nM)	120.33 ± 28.05	813.33 ± 34.70	1170 ± 140	No binding
N (sites)	0.44 ± 0.04	0.55 ± 0.06	1.48 ± 0.09	-
ΔH (kcal/mol)	-11.63 ± 0.26	-8.36 ± 0.24	-7.05 ± 0.36	-
-TΔS (kcal/mol)	2.19 ± 0.22	0.25 ± 0.53	-1.05 ± 0.38	-
ΔG (kcal/mol)	-9.46 ± 0.13	-8.31 ± 0.02	-8.10 ± 0.07	-

Titrations of DOPC LUVs (10 mM total lipid) containing 100 μM or 200 μM LII-D-Ala or LII-D-Lac. *Experiment performed by Ioli Kotsogianni.*

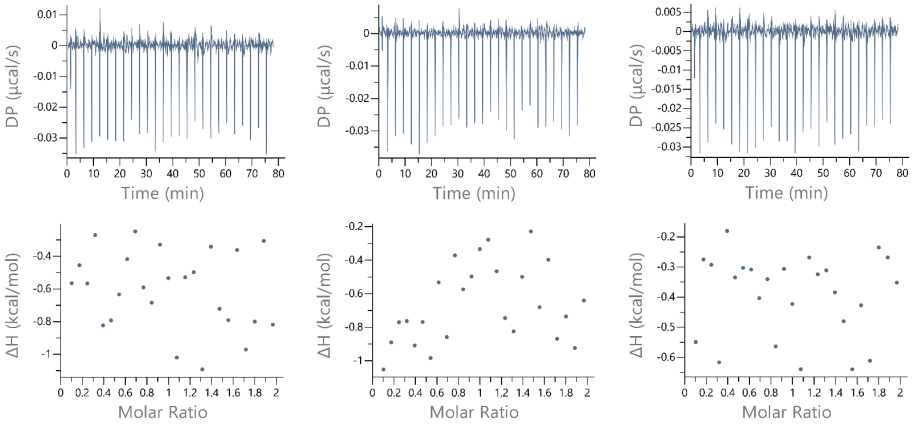

Fig. S3. Control ITC titrations of buffer titrated into vancomycin (10 μM). Titrations show the heat of dilution. n=3. *Experiment performed by Ioli Kotsogianni.*

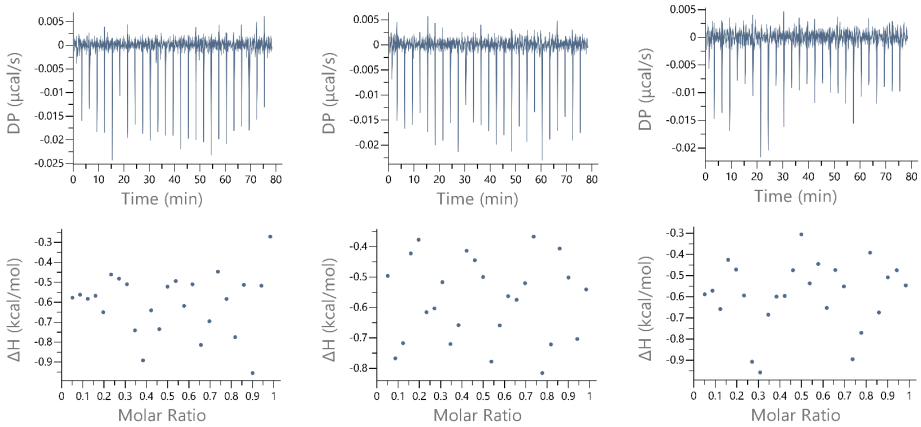

Fig. S4. Control ITC titrations of buffer titrated into compound 7 (20 µM). Control titrations show heat of dilution. n=3. *Experiment performed by Ioli Kotsogianni.*

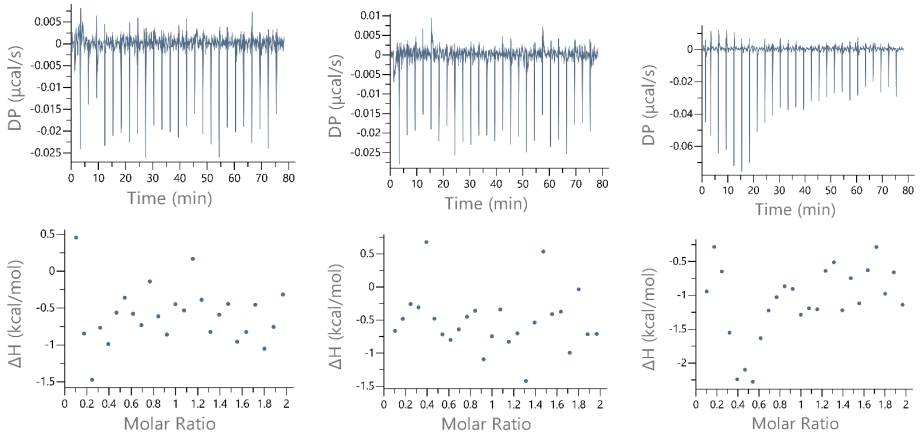

Fig. S5. Control ITC titrations of blank DOPC LUVs titrated into vancomycin (10 µM). Titrations show heat of dilution. n=3. *Experiment performed by Ioli Kotsogianni.*

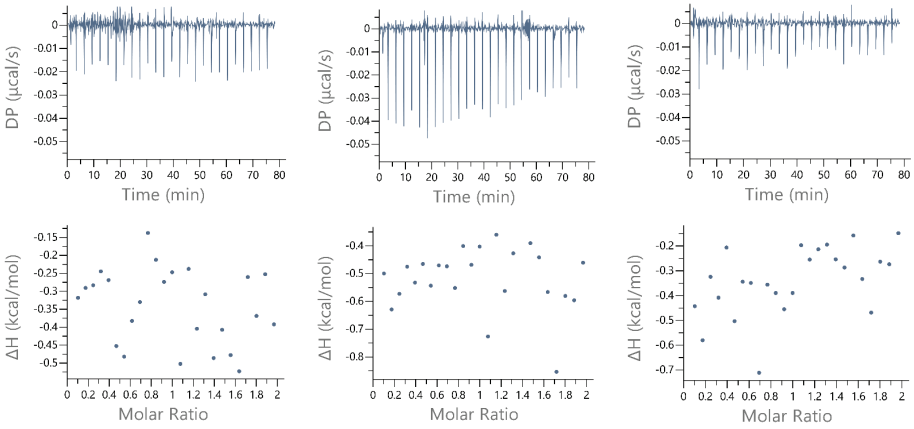

Fig. S6. Control ITC titrations of DOPC LUVs titrated into compound 7 (20 µM). Control titrations show heat of dilution. n=3. *Experiment performed by Ioli Kotsogianni.*

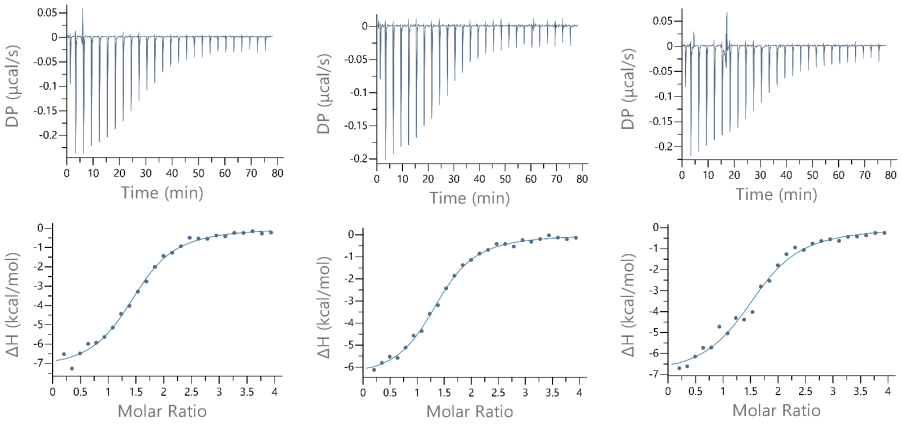

Fig. S7. Binding thermograms of 200 µM LII-D-Ala, 10 mM DOPC LUVs titrated into vancomycin (10 µM). n=3. *Experiment performed by Ioli Kotsogianni.*

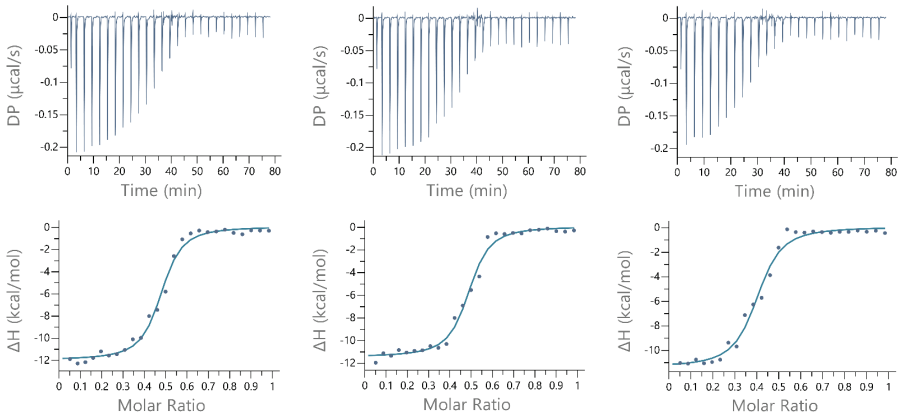

Fig. S8. Binding thermograms of 100 µM LII-D-Ala, 10 mM DOPC LUVs titrated into compound 7 (20 µM). n=3. *Experiment performed by Ioli Kotsogianni.*

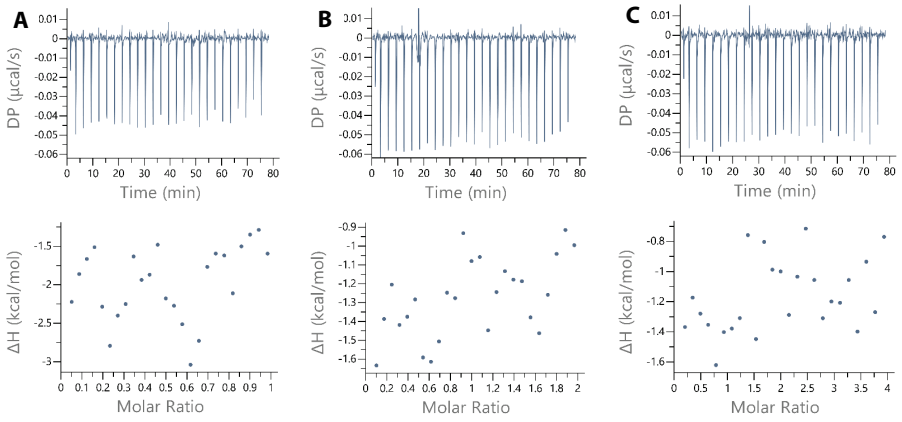

Fig. S9. Titrations of DOPC LUVs containing LII-D-Lac into vancomycin. Titrations produced negligible heat signals. (**A**) 1:3 DOPG/DOPC LUVs with 100 µM LII-D-Lac into vancomycin (20 µM). (**B**) DOPC LUVs with 200 µM LII-D-Lac into vancomycin (20 µM) and (**C**) DOPC LUVs with 200 µM LII-D-Lac into vancomycin (10 µM). *Experiment performed by Ioli Kotsogianni.*

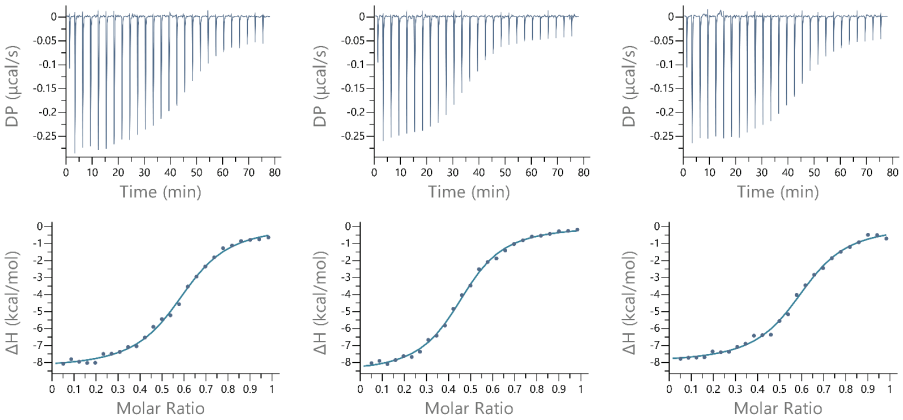

Fig. S10. Binding thermograms of 200 µM LII-D-Lac containing DOPC LUVs titrated into compound 7 (40 µM). n=3. *Experiment performed by Ioli Kotsogianni.*

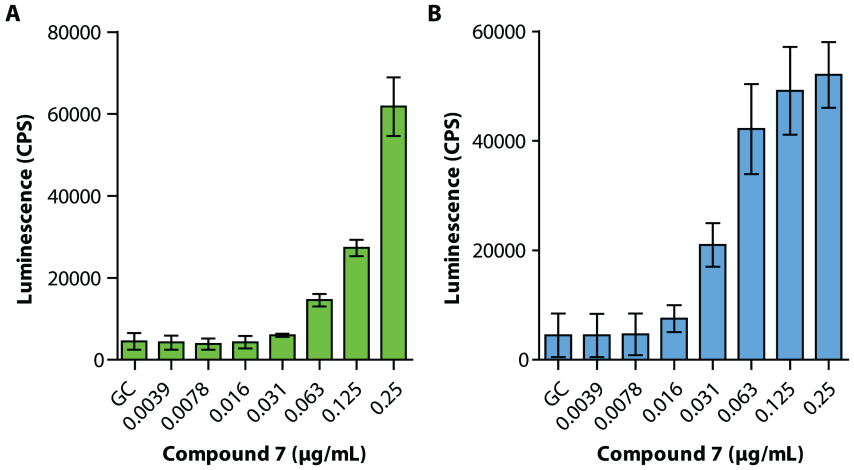

Fig. S11. Induction of the cell wall stress response. Induction of cell wall stress response after treatment of the (**A**) *S. aureus* VraRS-lux and (**B**) *B. subtilis* LiaI-lux bioreporter with increasing concentrations of compound **7**. Untreated cells were used as a growth control (GC). n=3. *Experiment performed by Melina Arts/Stefania De Benedetti.*

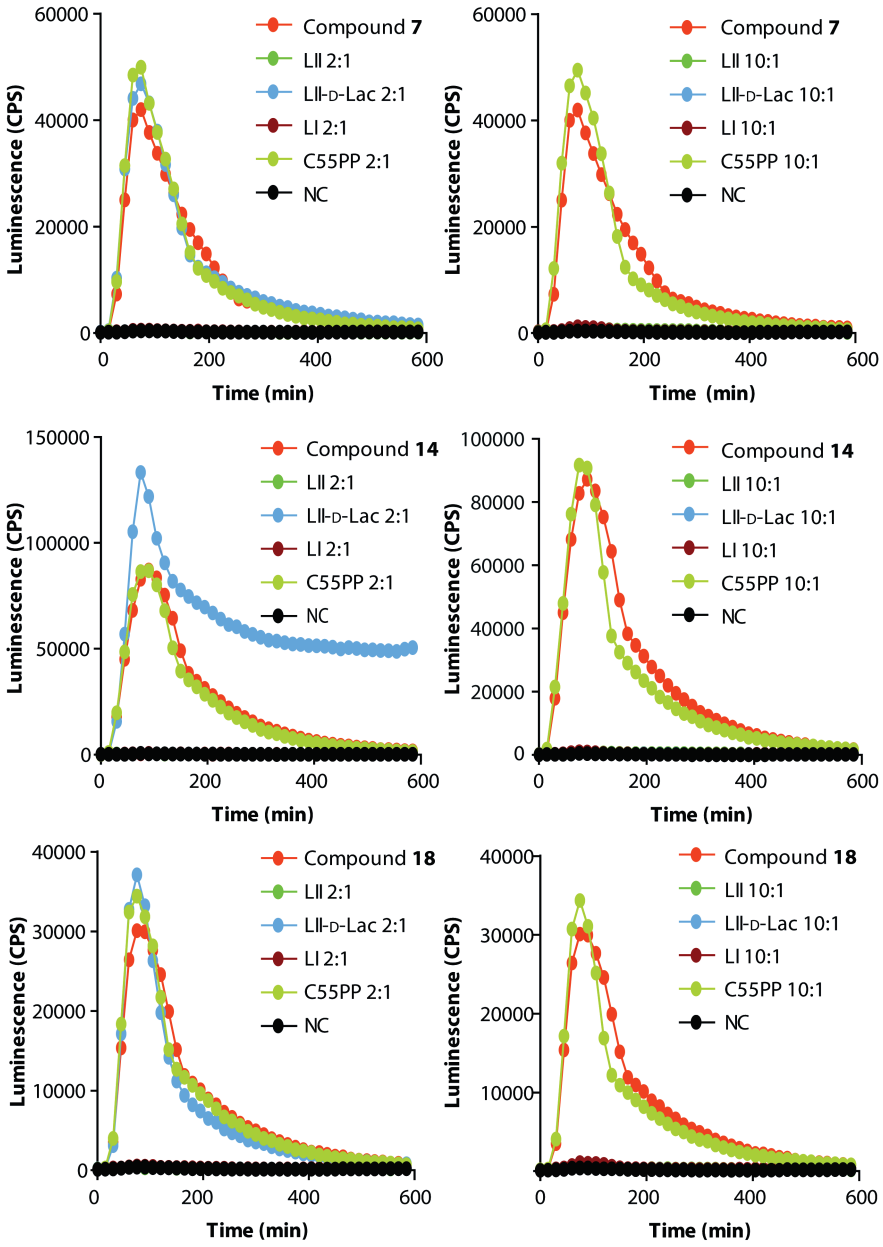

Fig. S12. Antagonization of cell wall stress response in *B. subtilis* by purified cell wall precursors. The lial-lux response triggered by compound **7**, **14,** and **18** is antagonized by lipid I (LI) and lipid II (LII) at two-fold molar access (left column), while a 10-fold molar excess of LII-D-Lac is required for full antagonization (right column). No antagonization is observed with C_{55}PP. *Experiment performed by Melina Arts/Stefania De Benedetti.*

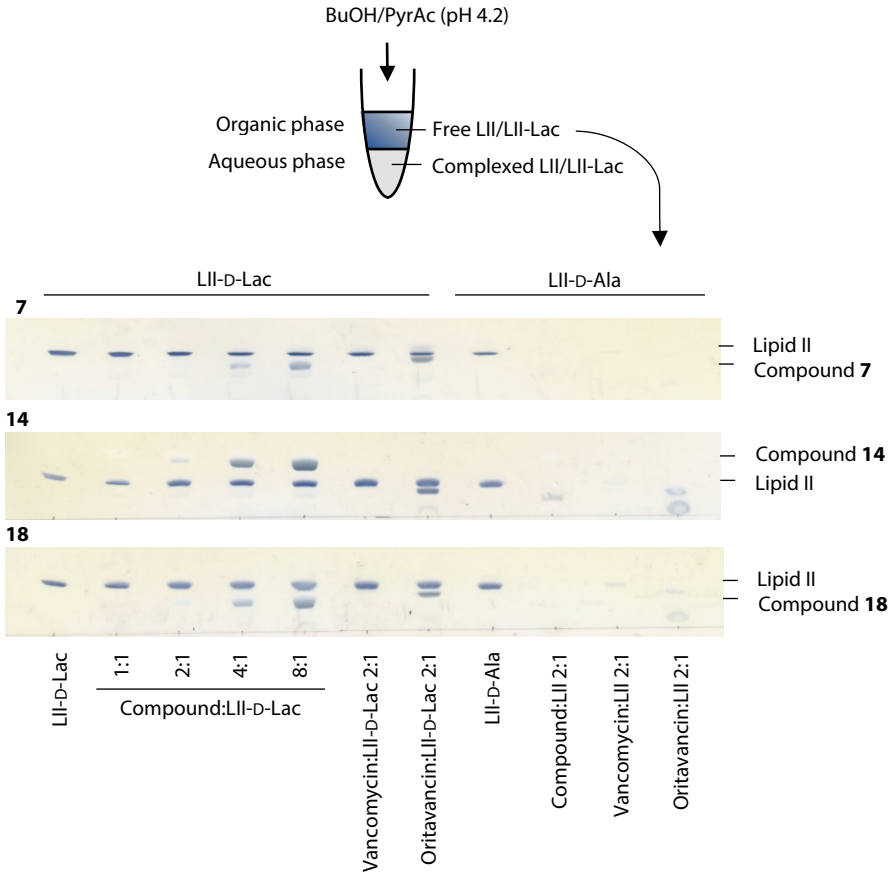

Fig. S13. Complex formation of compound 7, 14, and 18 with purified LII-D-Ala and LII-D-Lac. Compound **7**, **14,** and **18** were added to LII-D-Ala and LII-D-Lac at increasing molar ratios. Free lipids were extracted with BuOH/PyrAc and applied to TLC plates. The presence of extraction-stable complexes of all compounds with LII-D-Ala in the aqueous phase indicated by a reduction of the amount of LII visible on TLC. No complex formation with LII-D-Lac was observed similar to oritavancin and vancomycin. Image representative for technical replicates. *Experiment performed by Melina Arts/Stefania De Benedetti.*

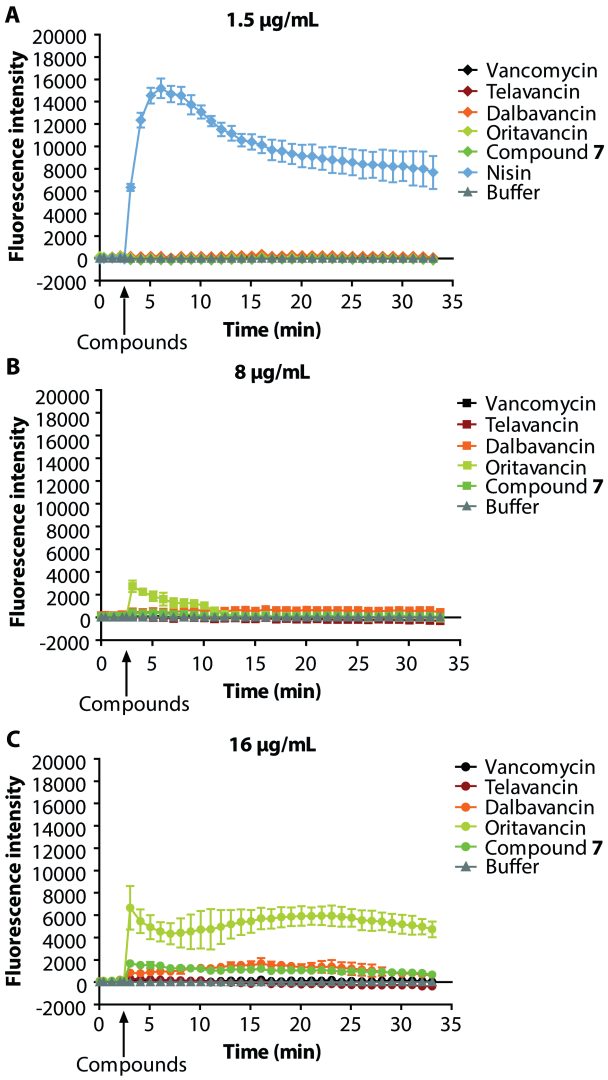

Fig. S14. Membrane depolarization assessment of the guanidino lipoglycopeptides. Fluorescence intensity of $diSC_3(5)$ released from the membrane of MRSA USA300 in the presence of antibiotic. $diSC_3(5)$ is a cationic fluorescent probe that accumulates on hyperpolarized membranes and translocates to the lipid bilayer. Upon disruption of the membrane potential, $diSC_3(5)$ can no longer partition to the cell surface, resulting in release of the dye into the media, which can be measured by an increase in fluorescence. After $diSC_3(5)$ and bacterial cells were incubated for 3 minutes, compounds were added, and a 30-minute time course was recorded. All data were normalized by subtraction of the signal derived from the buffer. Nisin at 1.5 µg/mL was used as positive control. Data are mean ± SD (n=3). (**A**) 30-minute time course of $diSC_3(5)$ fluorescence intensity of MRSA USA300 treated with nisin, vancomycin, telavancin, dalbavancin, oritavancin, and compound **7** at 1.5 µg/mL, (**B**) 8 µg/mL, and (**C**) 16 µg/mL.

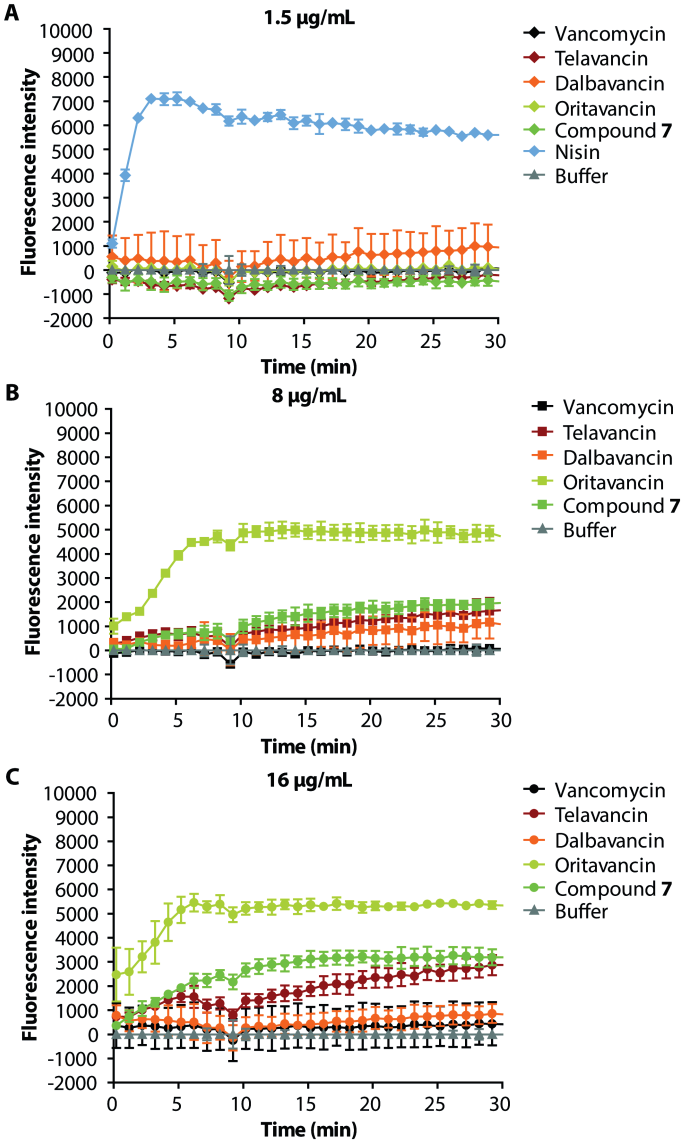

Fig. S15. Membrane pore formation assessment of the guanidino lipoglycopeptides. Fluorescence intensity of propidium iodide (PI) binding to DNA of MRSA USA300 in the presence of antibiotics was recorded in a 30-minute time course. PI is a red-fluorescent dye impermeable to live cells. Upon pore formation PI enters cells and binds DNA resulting in an increased fluorescence signal. All data were normalized by subtraction of the signal derived from the buffer. Nisin at 1.5 µg/mL was used as positive control. Data are mean ± SD (n=3). (**A**) 30-minute time course of PI fluorescence intensity of MRSA USA300 treated with nisin, vancomycin, telavancin, dalbavancin, oritavancin, and compound **7** at 1.5 µg/mL, (**B**) 8 µg/mL, and (**C**) 16 µg/mL.

Table S3. Extended mouse PK of guanidino lipoglycopeptide 7. Individual and mean/median mouse pharmacokinetic parameters of compound **7** (3 mg/kg, subcutaneous)

PK Parameter	Compound 7				
	Sample 1	Sample 2	Sample 3	Mean / Median	SD
C_0 / C_{max} (ng mL^{-1})	1989	1903	1546	1813	235
C_0 / C_{max} (nM)	1174	1123	912	1070	139
C_{last} (ng mL^{-1})	85.3	34.4	44.2	54.6	27.0
t_{last} (h)	8.00	8.00	8.00	8.00	-
t_{max} (h)	1.00	1.00	2.00	1.00	-
$t_{1/2}$ (h)	1.43	1.05	1.17	1.22	0.196
CL / CL_F (mL min^{-1} kg^{-1})	9	9	10	9.30	0.944
AUC_{inf} (ng hr mL^{-1})	5664	5759	4814	5412	520
AUC_{inf} (nM hr)	3342	3398	2841	3194	307
AUC_{0-t} (ng hr mL^{-1})	5487	5707	4740	5311	507
AUC_{0-t} (nM hr)	3238	3368	2797	3134	299
Number of Points used for Lambda z	3	3	3	3	-
AUC % Extrapolation to infinity	3.1	0.9	1.6	1.9	1.1

Table S4. Individual data of mouse thigh burden. Thigh burdens in colony forming units (CFU)/g. BLD= below limit of detection. q indicates dosing interval.

Pretreatment	Vehicle q6h	Vancomycin 25 mg/kg q12h	Compound 7 3 mg/kg q6h	Compound 7 10 mg/kg q6h
76075	488345865	106	42132	7984
80434	3971232877	825	7735	81
83111	555841584	1030	3885	34
86078	835263158	2023	113	368
90667	987022901	1148	368	35
100286	722195122	142564	456	77
73102	512903226	4605085	9139	96
85217	814594595	283390	666	76
121720	855384615	1204	350	40
73286	1851351351	310	587	BLD
89346	1471428571	BLD	75	158
110505	2851282051	6736	113	BLD

Table S5. Kruskal-Wallis statistical comparison of thigh burden. Corrected for multiple comparisons, StatsDirect-Conover-Inman. NS = not significant. q indicates dosing interval.

	Vehicle (SC, q6h)	**Compound 7 (3 mg/kg, SC, q6h)**	**Compound 7 (10 mg/kg, SC, q6h)**	**Vancomycin (25 mg/kg, IV, q12h)**
Pretreatment	p=0.004	p=0.0001	p<0.0001	p=0.0042
Vehicle (SC, q6h)		p<0.0001	p<0.0001	p<0.0001
Compound 7 (3 mg/kg, SC, q6h)			p=0.0001	NS
Compound 7 (10 mg/kg, SC, q6h)				p<0.0001
Vancomycin (25 mg/kg. IV, q12h)				

Table S6. Mean and Median survival. q indicates dosing interval.

	Mean survival (h)	**Median survival (h)**
Vehicle (SC, q6h)	51.3	50.7
Compound 7 (3 mg/kg, SC, q6h)	165.3	169.0
Compound 7 (10 mg/kg, SC, q6h)	169.0	169.0
Compound 7 (25mg/kg, IV, q12h)	169.0	169.0
Vancomycin (25 mg/kg, IV, q12h)	131.5	132.7

Table S7. Individual survival data of the mouse survival study. q indicates dosing interval.

Treatment	Animal number	Survival (h)	Survival (days)
Vehicle (SC, q6h)	1	49.4	2.1
	2	53.0	2.2
	3	46.0	1.9
	4	44.2	1.8
	5	56.5	2.4
	6	49.4	2.1
	7	50.7	2.1
	8	50.7	2.1
	9	56.5	2.4
	10	56.5	2.4
Compound 7 (3 mg/kg, SC, q6h)	11	132.2	5.5
	12	169.0	7.0
	13	169.0	7.0
	14	169.0	7.0
	15	169.0	7.0
	16	169.0	7.0
	17	169.0	7.0
	18	169.0	7.0
	19	169.0	7.0
	20	169.0	7.0
Compound 7 (10 mg/kg, SC, q6h)	21	169.0	7.0
	22	169.0	7.0
	23	169.0	7.0
	24	169.0	7.0
	25	169.0	7.0
	26	169.0	7.0
	27	169.0	7.0
	28	169.0	7.0
	29	169.0	7.0
	30	169.0	7.0
Compound 7 (25mg/kg, IV, q12h)	31	169.0	7.0
	32	169.0	7.0
	33	169.0	7.0
	34	169.0	7.0
	35	169.0	7.0
	36	169.0	7.0
	37	169.0	7.0
	38	169.0	7.0
	39	169.0	7.0
	40	169.0	7.0
Vancomycin (25 mg/kg, IV, q12h)	41	119.7	5.0
	42	153.5	6.4
	43	120.0	5.0
	44	133.0	5.5
	45	133.0	5.5
	46	132.4	5.5
	47	169.0	7.0
	48	81.0	3.4
	49	120.0	5.0
	50	153.5	6.4

Table S8. Statistical comparison of survival times. q indicates dosing interval.

Comparison	Log-rank test	Generalized Wilcoxon (Peto-Prentice)
Vehicle vs **7** (3 mg/kg, SC, q6h)	p<0.0001	p<0.0001
Vehicle vs **7** (10 mg/kg, SC, q6h)	p<0.0001	p<0.0001
Vehicle vs **7** (25 mg/kg, IV, q12h)	p<0.0001	p<0.0001
Vehicle vs vancomycin 25 mg/kg, IV, q12h)	p<0.0001	p<0.0001
Vancomycin (25 mg/kg, IV, q12h) vs **7** (25 mg/kg, IV, q12h)	p<0.0001	p=0.0001

Table S9. Individual data of mouse spleen burden. Burdens in colony forming units (CFU)/g. BLD= below limit of detection. q indicates dosing interval.

Pre-treatment	Vehicle (SC, q6h)	Compound 7 (10 mg/kg, SC, q6h)	Compound 7 (25 mg/kg, IV, q12h)	Vancomycin (25 mg/kg, IV, q12h)
14133333	26423	22705	1052	25650
16800000	25127	3688	5460	21700
12900000	8720	13997	2543	12218
14133333	26087	8720	7537	25554
15766667	20645	6596	2785	21317

Table S10. Kruskal-Wallis statistical comparison of spleen burden. Corrected for multiple comparisons, StatsDirect-Conover-Inman. NS = not significant. q indicates dosing interval.

	Vehicle (SC, q6h)	Compound 7 (10 mg/kg, SC, q6h)	Compound 7 (25 mg/kg, IV, q12h)	Vancomycin (25 mg/kg, IV, q12h)
Pretreatment	p=0.0029	p<0.0001	p<0.0001	p=0.0014
Vehicle (SC, q6h)		p=0.0059	p<0.0001	NS
Compound 7 (10 mg/kg, SC, q6h)			p=0.0054	p=0.0012
Compound 7 (25mg/kg, IV, q12h)				p<0.0001
Vancomycin (25 mg/kg, IV, q12h)				

Table S11. Individual data of mouse kidney burden. Burdens in colony forming units (CFU)/g. BLD= below limit of detection. q indicates dosing interval.

Pre-treatment	Vehicle (SC, q6h)	Compound 7 (10 mg/kg, SC, q6h)	Compound 7 (25 mg/kg, IV, q12h)	Vancomycin (25 mg/kg, IV, q12h)
30000	831818	BLD	BLD	452
33273	2102128	420	BLD	1268
27727	12400000	192	BLD	445
34571	11756098	BLD	526	53
23048	384324	BLD	BLD	53

Table S12. Kruskal-Wallis statistical comparison of kidney burden. Corrected for multiple comparisons, StatsDirect-Conover-Inman. NS = not significant. q indicates dosing interval.

	Vehicle (SC, q6h)	Compound 7 (10 mg/kg, SC, q6h)	Compound 7 (25 mg/kg, IV, q12h)	Vancomycin (25 mg/kg, IV, q12h)
Pretreatment	NS	p=0.0002	p<0.0001	NS
Vehicle (SC, q6h)		p<0.0001	p<0.0001	p=0.0019
Compound 7 (10 mg/kg, SC, q6h)			NS	p=0.0287
Compound 7 (25mg/kg, IV, q12h)				p=0.0096
Vancomycin (25 mg/kg, IV, q12h)				

Table S13. Individual data of mouse heart burden. Burdens in colony forming units (CFU)/g. BLD= below limit of detection. q indicates dosing interval.

Pre-treatment	Vehicle (SC, q6h)	Compound 7 (10 mg/kg, SC, q6h)	Compound 7 (25 mg/kg, IV, q12h)	Vancomycin (25 mg/kg, IV, q12h)
1090	459	BLD	BLD	BLD
9366	848	BLD	BLD	675
4149	330	BLD	BLD	BLD
11488	4127	164	14746	BLD
10530	1787059	BLD	BLD	128

Table S14. Kruskal-Wallis statistical comparison of heart burden. Corrected for multiple comparisons, StatsDirect-Conover-Inman. NS = not significant. q indicates dosing interval.

	Vehicle (SC, q6h)	Compound 7 (10 mg/kg, SC, q6h)	Compound 7 (25 mg/kg, IV, q12h)	Vancomycin (25 mg/kg, IV, q12h)
Pretreatment	NS	p=0.0011	p=0.0037	p=0.005
Vehicle (SC, q6h)		p=0.005	p=0.0152	p=0.0203
Compound 7 (10 mg/kg, SC, q6h)			NS	NS
Compound 7 (25mg/kg, IV, q12h)				NS
Vancomycin (25 mg/kg, IV, q12h)				

References

1. Murray, C. J. L., *et al.* Global burden of bacterial antimicrobial resistance in 2019: a systematic analysis. *Lancet* **399**, 629–655 (2022).
2. Pootoolal, J., Neu, J. & Wright, G. D. Glycopeptide Antibiotic Resistance. *Annu. Rev. Pharmacol. Toxicol.* **42**, 381–408 (2002).
3. Walsh, C. T., Fisher, S. L., Park, I. S., Prahalad, M. & Wu, Z. Bacterial resistance to vancomycin: Five genes and one missing hydrogen bond tell the story. *Chem. Biol.* **3**, 21–28 (1996).
4. Blaskovich, M. A. T., *et al.* Developments in Glycopeptide Antibiotics. *ACS Infect. Dis.* **4**, 715–735 (2018).
5. Barna, J. C. & Williams, D. H. The structure and mode of action of glycopeptide antibiotics of the vancomycin group. *Annu. Rev. Microbiol.* **38**, 339–357 (1984).
6. McComas, C. C., Crowley, B. M. & Boger, D. L. Partitioning the Loss in Vancomycin Binding Affinity for d-Ala-d-Lac into Lost H-Bond and Repulsive Lone Pair Contributions. *J. Am. Chem. Soc.* **125**, 9314–9315 (2003).
7. Bugg, T. D. H., *et al.* Molecular basis for vancomycin resistance in Enterococcus faecium BM4147: biosynthesis of a depsipeptide peptidoglycan precursor by vancomycin resistance proteins VanH and VanA. *Biochemistry* **30**, 10408–10415 (1991).
8. Arthur, M. & Quintiliani, R. Regulation of VanA-and VanB-type glycopeptide resistance in enterococci. *Antimicrob. Agents Chemother.* **45**, 375–381 (2001).
9. Courvalin, P. Resistance of enterococci to glycopeptides. *Antimicrob. Agents Chemother.* **34**, 2291–2296 (1990).
10. Wanat, K. Biological barriers, and the influence of protein binding on the passage of drugs across them. *Mol. Biol. Rep.* **47**, 3221–3231 (2020).
11. Lee, B. L., Sachdeva, M. & Chambers, H. F. Effect of protein binding of daptomycin on MIC and antibacterial activity. *Antimicrob. Agents Chemother.* **35**, 2505–2508 (1991).
12. Lister, J. L. & Horswill, A. R. Staphylococcus aureus biofilms: recent developments in biofilm dispersal. *Front. Cell. Infect. Microbiol.* **4**, 178 (2014).
13. Sanchez, C. J., *et al.* Biofilm formation by clinical isolates and the implications in chronic infections. *BMC Infect. Dis.* **13**, 47 (2013).
14. Di Domenico, E. G., *et al.* Microbial biofilm correlates with an increased antibiotic tolerance and poor therapeutic outcome in infective endocarditis. *BMC Microbiol.* **19**, 228 (2019).
15. Rodríguez-Lázaro, D., *et al.* Characterization of Biofilms Formed by Foodborne Methicillin-Resistant Staphylococcus aureus. *Front. Microbiol.* **9**, (2018).
16. Reynolds, P. E. Studies on the mode of action of vancomycin. *Biochim. Biophys. Acta* **52**, 403–405 (1961).
17. Somner, E. A. & Reynolds, P. E. Inhibition of peptidoglycan biosynthesis by ramoplanin. *Antimicrob. Agents Chemother.* **34**, 413–419 (1990).
18. Siewert, G. & Strominger, J. L. Bacitracin: an inhibitor of the dephosphorylation of lipid pyrophosphate, an intermediate in the biosynthesis of the peptidoglycan of bacterial cell walls. *Proc. Natl. Acad. Sci.* **57**, 767–773 (1967).
19. Breukink, E. & de Kruijff, B. Lipid II as a target for antibiotics. *Nat. Rev. Drug Discov.* **5**, 321–323 (2006).
20. Beauregard, D. A., Williams, D. H., Gwynn, M. N. & Knowles, D. J. C. Dimerization and membrane anchors in extracellular targeting of vancomycin group antibiotics. *Antimicrob. Agents Chemother.* **39**, 781–785 (1995).
21. Mackay, J. P., *et al.* Glycopeptide Antibiotic Activity and the Possible Role of Dimerization: A Model for Biological Signaling. *J. Am. Chem. Soc.* **116**, 4581–4590 (1994).
22. Mascher, T., Zimmer, S. L., Smith, T.-A. & Helmann, J. D. Antibiotic-inducible promoter regulated by the cell envelope stress-sensing two-component system LiaRS of Bacillus subtilis. *Antimicrob. Agents Chemother.* **48**, 2888–2896 (2004).
23. Radeck, J., *et al.* Anatomy of the bacitracin resistance network in Bacillus subtilis. *Mol. Microbiol.* **100**, 607–620 (2016).
24. Tan, S., Ludwig, K. C., Müller, A., Schneider, T. & Nodwell, J. R. The Lasso Peptide Siamycin-I Targets Lipid II at the Gram-Positive Cell Surface. *ACS Chem. Biol.* **14**, 966–974 (2019).
25. Münch, D., *et al.* Structural Variations of the Cell Wall Precursor Lipid II and Their Influence on Binding and Activity of the Lipoglycopeptide Antibiotic Oritavancin. *Antimicrob. Agents*

Chemother. **59**, 772–781 (2015).
26. Beauregard, D. A., Williams, D. H., Gwynn, M. N. & Knowles, D. J. Dimerization and membrane anchors in extracellular targeting of vancomycin group antibiotics. *Antimicrob. Agents Chemother.* **39**, 781–785 (1995).
27. Van Bambeke, F. Lipoglycopeptide Antibacterial Agents in Gram-Positive Infections: A Comparative Review. *Drugs* **75**, 2073–2095 (2015).
28. Kahne, D., Leimkuhler, C., Lu, W. & Walsh, C. Glycopeptide and Lipoglycopeptide Antibiotics. *Chem. Rev.* **105**, 425–448 (2005).
29. Hurdle, J. G., O'Neill, A. J., Chopra, I. & Lee, R. E. Targeting bacterial membrane function: An underexploited mechanism for treating persistent infections. *Nat. Rev. Microbiol.* **9**, 62–75 (2011).
30. Jay Sims, P., Waggoner, A. S., Wang, C.-H. & Hoffman, J. F. Studies on the Mechanism by Which Cyanine Dyes Measure Membrane Potential in Red Blood Cells and Phosphatidylcholine Vesicles. *Biochemistry* **13**, 3315–3330 (1974).
31. Belley, A., *et al.* Oritavancin Disrupts Membrane Integrity of Staphylococcus aureus and Vancomycin-Resistant Enterococci To Effect Rapid Bacterial Killing. *Antimicrob. Agents Chemother.* **54**, 5369–5371 (2010).
32. Belley, A., *et al.* Oritavancin Kills Stationary-Phase and Biofilm Staphylococcus aureus Cells In Vitro. *Antimicrob. Agents Chemother.* **53**, 918–925 (2009).
33. Arndt-Jovin, D. J. & Jovin, T. M. Fluorescence Labeling and Microscopy of DNA. *Methods Cell Biol.* **30**, 417–448 (1989).
34. Strahl, H. & Hamoen, L. W. Membrane potential is important for bacterial cell division. *Proc. Natl. Acad. Sci.* **107**, 12281–12286 (2010).
35. Payne, D. J., Gwynn, M. N., Holmes, D. J. & Pompliano, D. L. Drugs for bad bugs: Confronting the challenges of antibacterial discovery. *Nat. Rev. Drug Discov.* **6**, 29–40 (2007).
36. Gudmundsson, S. & Erlendsdóttir, H. Chapter 15 - Murine Thigh Infection Model. in *Handbook of Animal Models of Infection* (eds. Zak, O. & Sande, M. A.) 137–144 (Academic Press, 1999).
37. Vincent, L. L. & Otto, C. M. Infective Endocarditis: Update on Epidemiology, Outcomes, and Management. *Curr. Cardiol. Rep.* **20**, 86 (2018).
38. Durante-Mangoni, E., *et al.* Dalbavancin for infective endocarditis: a single centre experience. *J. Chemother.* **33**, 256–262 (2021).
39. Ajaka, L., Heil, E. & Schmalzle, S. Dalbavancin in the Treatment of Bacteremia and Endocarditis in People with Barriers to Standard Care. *Antibiot. (Basel, Switzerland)* **9**, 700 (2020).
40. Steele, J. M., Seabury, R. W., Hale, C. M. & Mogle, B. T. Unsuccessful treatment of methicillin-resistant Staphylococcus aureus endocarditis with dalbavancin. *J. Clin. Pharm. Ther.* **43**, 101–103 (2018).
41. Kussmann, M., *et al.* Emergence of a dalbavancin induced glycopeptide/lipoglycopeptide non-susceptible Staphylococcus aureus during treatment of a cardiac device-related endocarditis. *Emerg. Microbes Infect.* **7**, 1–10 (2018).
42. Centers for Disease Control (US). *Antibiotic Resistance Threats in the United States, 2019*. www.cdc.gov/DrugResistance/Biggest-Threats.html. (2019).
43. WHO. *Antimicrobial Resistance Global Report on Surveillance*. (2014).
44. Kavanagh, A., Ramu, S., Gong, Y., Cooper, M. A. & Blaskovich, M. A. T. Effects of Microplate Type and Broth Additives on Microdilution MIC Susceptibility Assays. *Antimicrob. Agents Chemother.* **63**, e01760-18 (2021).
45. Schmidt, S., *et al.* Effect of Protein Binding on the Pharmacological Activity of Highly Bound Antibiotics. *Antimicrob. Agents Chemother.* **52**, 3994–4000 (2008).
46. Arhin, F. F., *et al.* Assessment of oritavancin serum protein binding across species. *Antimicrob. Agents Chemother.* **54**, 3481–3483 (2010).
47. Greenblatt, D. J., Sellers, E. M. & Koch-Weser, J. Importance of protein binding for the interpretation of serum or plasma drug concentrations. *J. Clin. Pharmacol.* **22**, 259–263 (1982).
48. Merrikin, D. J., Briant, J. & Rolinson, G. N. Effect of protein binding on antibiotic activity in vivo. *J. Antimicrob. Chemother.* **11**, 233–238 (1983).
49. Bailey, E. M., Rybak, M. J. & Kaatz, G. W. Comparative Effect of Protein Binding on the Killing Activities of Teicoplanin and Vancomycin. *Antimicrob. Agents Chemother.* **35**, 1089–1092 (1991).
50. Belley, A., Seguin, D. L., Arhin, F. & Moeck, G. Comparative In Vitro Activities of Oritavancin, Dalbavancin, and Vancomycin against Methicillin-Resistant Staphylococcus aureus Isolates in a Nondividing State. *Antimicrob. Agents Chemother.* **60**, 4342–4345 (2016).
51. Innovotech Inc. *The MBEC Physiology & Genetics assay: instruction manual*. (2008).

52. Schneider, T., *et al.* Plectasin, a Fungal Defensin, Targets the Bacterial Cell Wall Precursor Lipid II. *Science* **328**, 1168–1172 (2010).
53. Schneider, T., *et al.* In vitro assembly of a complete, pentaglycine interpeptide bridge containing cell wall precursor (lipid II-Gly5) of Staphylococcus aureus. *Mol. Microbiol.* **53**, 675–685 (2004).
54. Müller, A., *et al.* Lipodepsipeptide empedopeptin inhibits cell wall biosynthesis through Ca2+-dependent complex formation with peptidoglycan precursors. *J. Biol. Chem.* **287**, 20270–20280 (2012).
55. Ling, L. L., *et al.* A new antibiotic kills pathogens without detectable resistance. *Nature* **517**, 455 (2015).
56. Rick, P. D., *et al.* Characterization of the lipid-carrier involved in the synthesis of enterobacterial common antigen (ECA) and identification of a novel phosphoglyceride in a mutant of Salmonella typhimurium defective in ECA synthesis. *Glycobiology* **8**, 557–567 (1998).
57. Grein, F., *et al.* Ca2+-Daptomycin targets cell wall biosynthesis by forming a tripartite complex with undecaprenyl-coupled intermediates and membrane lipids. *Nat. Commun.* **11**, 1455 (2020).
58. Münch, D., *et al.* Identification and in vitro analysis of the GatD/MurT enzyme-complex catalyzing lipid II amidation in Staphylococcus aureus. *PLoS Pathog.* **8**, e1002509 (2012).
59. Müller, A., *et al.* Daptomycin inhibits cell envelope synthesis by interfering with fluid membrane microdomains. *Proc. Natl. Acad. Sci.* **113**, E7077–E7086 (2016).